

## Accepted Manuscript

Chlorinated Tacrine Analogs: Design, Synthesis and Biological Evaluation of Their Anti-cholinesterase Activity as Potential Treatment for Alzheimer's Disease

Hanan.M. Ragab, Mohamed Teleb, Hassan R. Haidar, Noha Gouda

PII: S0045-2068(18)31168-4

DOI: <https://doi.org/10.1016/j.bioorg.2019.02.033>

Reference: YBIOO 2808

To appear in: *Bioorganic Chemistry*

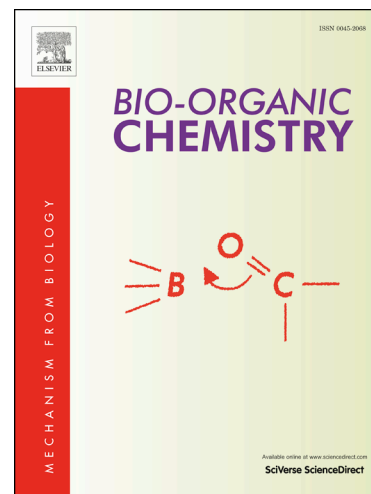
Received Date: 13 October 2018

Revised Date: 13 February 2019

Accepted Date: 13 February 2019

Please cite this article as: Hanan.M. Ragab, M. Teleb, H.R. Haidar, N. Gouda, Chlorinated Tacrine Analogs: Design, Synthesis and Biological Evaluation of Their Anti-cholinesterase Activity as Potential Treatment for Alzheimer's Disease, *Bioorganic Chemistry* (2019), doi: <https://doi.org/10.1016/j.bioorg.2019.02.033>

This is a PDF file of an unedited manuscript that has been accepted for publication. As a service to our customers we are providing this early version of the manuscript. The manuscript will undergo copyediting, typesetting, and review of the resulting proof before it is published in its final form. Please note that during the production process errors may be discovered which could affect the content, and all legal disclaimers that apply to the journal pertain.



## Chlorinated Tacrine Analogs: Design, Synthesis and Biological Evaluation of Their Anti-cholinesterase Activity as Potential Treatment for Alzheimer's Disease

Hanan. M. Ragab<sup>a\*</sup>, Mohamed Teleb<sup>a</sup>, Hassan R. Haidar<sup>b</sup>, Noha Gouda<sup>c</sup>

<sup>a</sup>Department of Pharmaceutical Chemistry, Faculty of Pharmacy, Alexandria University, Alexandria 21521, Egypt, <sup>b</sup> Hassan R. Haidar; Department of Pharmacology and Therapeutics, Faculty of Pharmacy, Beirut Arab University, Beirut, Lebanon, <sup>c</sup> Noha Gouda; Department of Pharmaceutics, Faculty of Pharmacy, Alexandria University, Alexandria 21521, Egypt

\* **Corresponding author details:** Hanan. M. Ragab(✉); Department of Pharmaceutical Chemistry, Faculty of Pharmacy, Alexandria University, Alexandria 21521, Egypt. E-mail: [tafida12@yahoo.com](mailto:tafida12@yahoo.com). Tel.: +20 1002646716, Fax: +20 34873273.

**Abstract:** In search of potent acetyl cholinesterase inhibitors with low hepatotoxicity for the treatment of Alzheimer's disease, introduction of a chloro substitution to tacrine and some of its analogs has proven to be beneficial in maintaining or potentiating the cholinesterase inhibitory activity. Furthermore, it was found to be able to reduce the hepatotoxicity of the synthesized compounds, which is the main target of the study. Accordingly, a series of new 4-(chlorophenyl)tetrahydroquinoline derivatives, was synthesized and characterized. The synthesized compounds were evaluated for their *in vitro* and *in vivo* anti-cholinesterase activity using tacrine as a reference standard. Furthermore, they were investigated for their hepatotoxicity compared to tacrine. The obtained biological results revealed that all synthesized compounds displayed equivalent or significantly higher anti-cholinesterase activity and lower hepatotoxicity in comparison to tacrine. In addition, *in silico* drug-likeness of the synthesized compounds were predicted and their practical logP were assessed indicating that all synthesized compounds can be considered as promising hits/leads. Furthermore, docking study of the compound showing the highest *in vitro* anticholinesterase activity was performed and its binding mode was compared to that of tacrine.

**Key words:** Alzheimer's disease, anti-cholinesterase activity, tacrine, chlorinated phenyl tetrahydroquinolines, hepatotoxicity.

**Funding:** The research did not receive any specific grant from funding agencies in the public, commercial, or not-for-profit sectors.

## 1. Introduction:

Alzheimer's disease (AD) is an age-related chronic neurodegenerative disorder occurring in middle or late life [1-4]. The disease is associated with progressive dementia leading to severe disability in performing the daily life activities [5]. Memory deterioration, loss of cognitive function and privation of personality are common symptoms of the disease [6]. AD is progressive and irreversible leading to abnormal changes in the brain that interferes with many aspects of brain functions and worsens over time [7]. AD progresses in stages ranging from mild forgetfulness and cognitive impairment to great loss of mental abilities. In highly advanced stages of AD, the patient becomes helpless and dependant on others for aspects of everyday life activities [8]. A family history may play a role in increasing one's risk of developing AD [9]. Postmortem brain tissue samples from AD patients revealed progressive accumulation of  $\beta$ -amyloid proteins ( $A\beta$ ) together with tau ( $\tau$ )-protein aggregation leading to shrinkage and death of neurons [10, 11]. Several theories have been proposed to explain the mechanism of AD development [12, 13], among which the cholinergic hypothesis has become the most leading theory to explain the etiology of the disease. This was based on the observation of cholinergic neurons loss in the brain area involved in cognitive and behavioral functions of AD patients. Furthermore, several centrally active anticholinergic drugs were found to induce dose-related cognitive deficits in humans [14]. Accordingly, increasing levels of acetylcholine (ACh) in cholinergic synapses in the brain of AD patients would be expected to relieve symptoms associated with the disease [15-18]. Consequently, inhibition of acetyl cholinesterase (AChE), the enzyme responsible for the hydrolysis of acetylcholine, has become the most targeted approach for the development of agents active against AD [19-24]. However, it is well established that the use of acetyl cholinesterase inhibitors (AChEIs) for the treatment of AD can only alleviate the symptoms. Unfortunately no clinically approved drug has been discovered that can reverse the progress of the disease.

Tacrine (9-amino-1,2,3,4-tetrahydroacridine) (**I**, Fig. 1) was the first AChEI to be approved by the Food and Drug Administration (FDA) for the treatment of AD [25-28]. However, despite its good AChE inhibitory activity, tacrine was far from ideal due to its low bioavailability and short half-life. Furthermore, frequent administration of tacrine was found to be associated with significant hepatotoxicity [29, 30]. Accordingly, several structural modifications were performed on tacrine aiming at producing potent AChEIs (equivalent to or more potent than tacrine) with minimum hepatotoxic side effects to provide clinically advantageous drugs [5]. Among the accomplished structural modifications, introduction of a chloro substitution to the phenyl ring of tacrine resulted into a group of chlorinated tetrahydroacridines (THA) (**II**, Fig. 1) showing high AChE inhibitory activity [31, 32].

One other successful structural modification which was affected in our laboratories, was the design and synthesis of a group of 3-cyano-2-substituted tetrahydroquinolines having a phenyl ring at the 4-position (**III**, Fig. 1). Structure-activity relationship (SAR) studies of these compounds indicated that the presence of a chloro substituent at the 2-position of the pyridine ring resulted in a lead compound that was more potent AChEI and less hepatotoxic than tacrine [1, 5]. Furthermore, studying the significance of the chloro substitution in tacrine analogs, Ragab et al. have previously synthesized two series of 4-phenyltetrahydroquinolines (**IV**; X = H, Cl, Fig. 1) and evaluated their anti-cholinesterase activity and hepatotoxicity. The chlorinated compounds (**IV**; X = Cl) showed higher AChE inhibitory activity and lower hepatotoxicity relative

to the unchlorinated analogs (**IV**; X = H) [5]. Correlating all the previously mentioned results, it was obvious that the presence of a chloro group on any of the aryl rings, whether pyridyl or phenyl, present in the synthesized tetrahydroquinolines (THQ) resulted in potent AChEIs with lower hepatotoxicity [5].

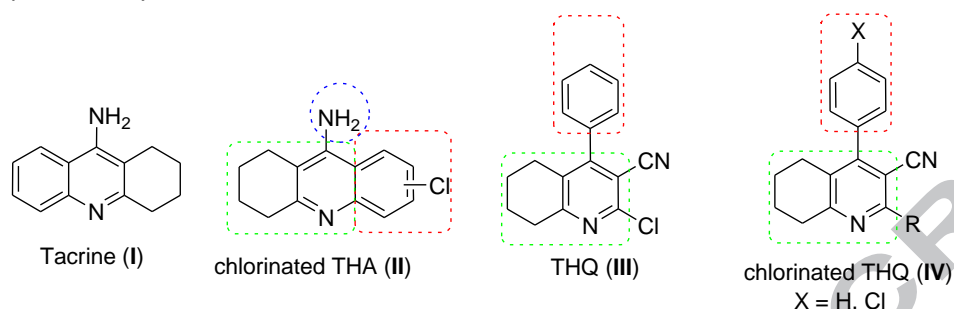


**Figure 1:** Chemical structure of tacrine (**I**), chlorinated tacrine (**II**), 2-chlorotetrahydroquinoline (**III**), 4-aryltetrahydroquinoline (THQ; **IV**).

Further investigation of the synthesized chlorinated THQ compounds (**IV** where X=Cl) revealed that nature of the substituent at the 2-position was found to possess great influence on the AChE inhibitory activity and the hepatotoxicity of the products. Presence of an amino group, whether free or mono substituted, at the 2-position (**V**;  $R_1$  = alkyl and  $R_2$  = H, Fig. 2) resulted into compounds having the highest AChE inhibitory activity and least hepatotoxicity. However, the introduction of a second alkyl substituent on the 2-amino group (**V**;  $R_1$  =  $R_2$  = alkyl, Fig. 2) totally abolished the activity. Furthermore, fusing the pyridine ring to a pyrazolo nucleus (**VI**, Fig. 2) resulted in a promising activity [5].

In addition, in a trial to improve AChE activity and decrease hepatotoxicity, Reddy et al. introduced an amide moiety in the form of acidhydrazide at the 2-position of tacrine (**VII**, Fig. 2). The produced compound was found to be totally safe implying that the introduction of an amide group might be beneficial[33].

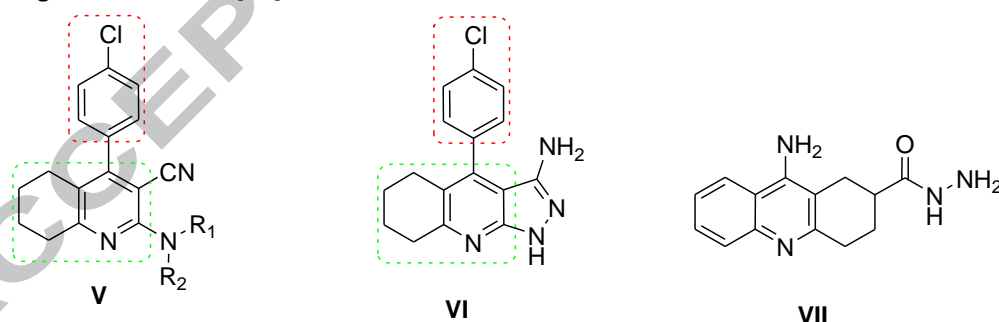


**Figure 2:** Chemical structure of 2-alkylamino-3-cyano-4-(p-chlorophenyl)tetrahydroquinolines (**V**) and 4-(p-chlorophenyl)pyrazolo[3,4-b]tetrahydroquinoline (**VI**) and 2-carbohydrazide derivative of tacrine (**VII**).

As an investment of the aforementioned findings, a novel group of chlorinated-2-amino-THQ derivatives with various functionalities and/or fused to different heterocyclic ring systems (**VIII** and **IX**, Fig. 3) was synthesized and evaluated for their AChE inhibitory activity and hepatotoxicity aiming at discovering potential potent AChEIs with lower (if any) hepatotoxicity than tacrine. The substitution pattern of the synthesized compounds was carefully chosen so as to examine the effect of different N-substituents at the 2-position having various electronic and lipophilic characters (**VIII**, Fig. 3). Furthermore, the effect of introduction of an amide group at the 2- and 3-positions of the synthesized analogs has been investigated. In addition, in case of

fused heterocycles (**IX**, Fig. 3), it was targeted to study how increasing the size of the ring fused to the pyridine ring; a pyrimidine rather than a pyrazole, would affect the biological results of the synthesized compounds.

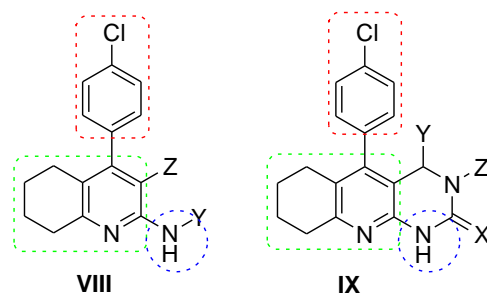


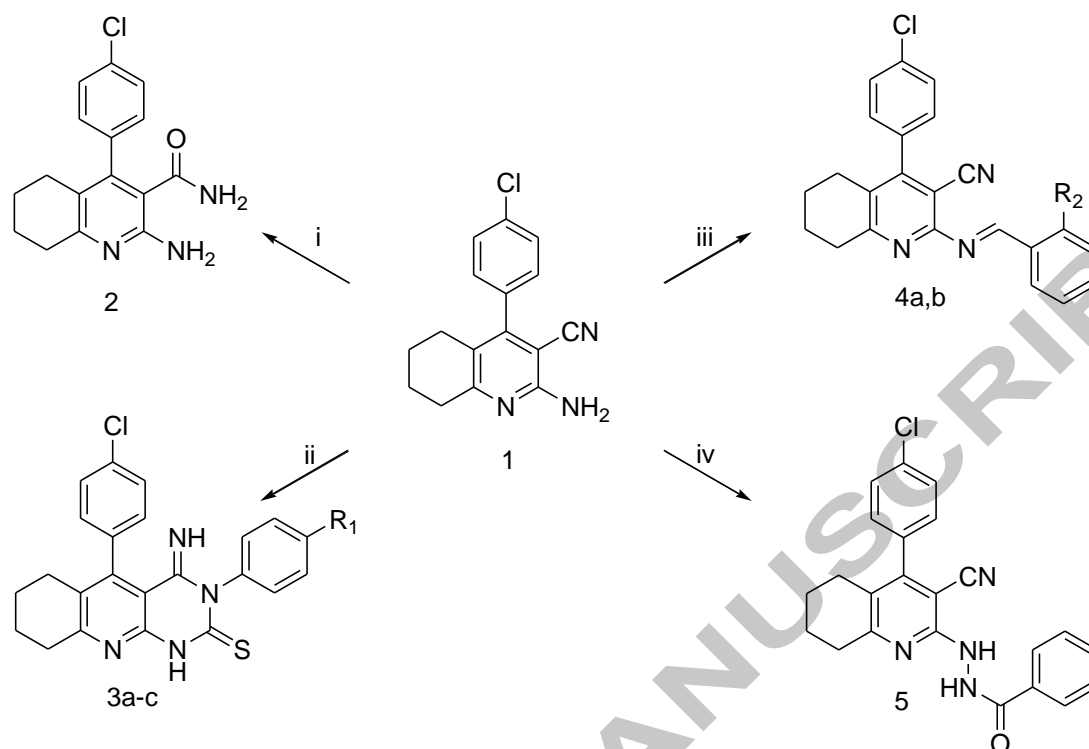
**Figure 3:** Newly designed 2-alkylamino-4-(p-chlorophenyl)tetrahydroquinolines (**VIII**) and 5-(p-chlorophenyl)pyrimido[4,5-b]tetrahydroquinoline (**IX**).

Furthermore, *in silico* physicochemical characters and pharmacokinetic parameters for the synthesized compounds were predicted using dedicated computer software [34-36] to ensure successful *in vivo* therapeutic activity. Practical logP testing was performed and compared to the theoretical values obtained. Finally, a docking study of compound **7** (the most *in vitro* active compound) was performed and its binding mode was compared to that of tacrine.

## 2. Results and discussion

### 2.1. Chemistry

The proposed synthetic routes adopted to obtain the target compounds are illustrated in Fig.4-6. In Fig. 4, the 2-amino-4-(4-chlorophenyl)-5,6,7,8-tetrahydroquinoline-3-carboxamide (**2**) was synthesized through hydrolysis of its 3-cyano precursor (**1**) upon heating on a water bath with 70% sulfuric acid according to a reported procedure [37, 38]. In addition, reaction of the 2-amino-3-cyano analog (**1**) with the appropriate aryl isothiocyanates resulted in the corresponding substituted tricyclic thiones (**3a-c**) instead of the expected open chain thiourea derivative. The cyclization of the obtained products was proven by their IR spectra which were missing the CN absorption band. The spectra also possessed new absorption bands for the C=S group. Furthermore,  $^{13}\text{C}$ -NMR of the synthesized derivatives indicated the appearance of a signal at  $\delta$  above 180 ppm corresponding to the C=S. Condensation of **1** with the appropriate aromatic aldehydes yielded the corresponding Schiff's bases (**4a, b**) which lacked the  $\text{NH}_2$  absorption bands present in its starting material. Finally, reaction of **1** with benzoic acid hydrazide in pyridine resulted in the benzoylhydrazide derivative (**5**) with its IR spectrum showing the absorption bands corresponding to both the carbonyl and NH-NH of the hydrazide group.

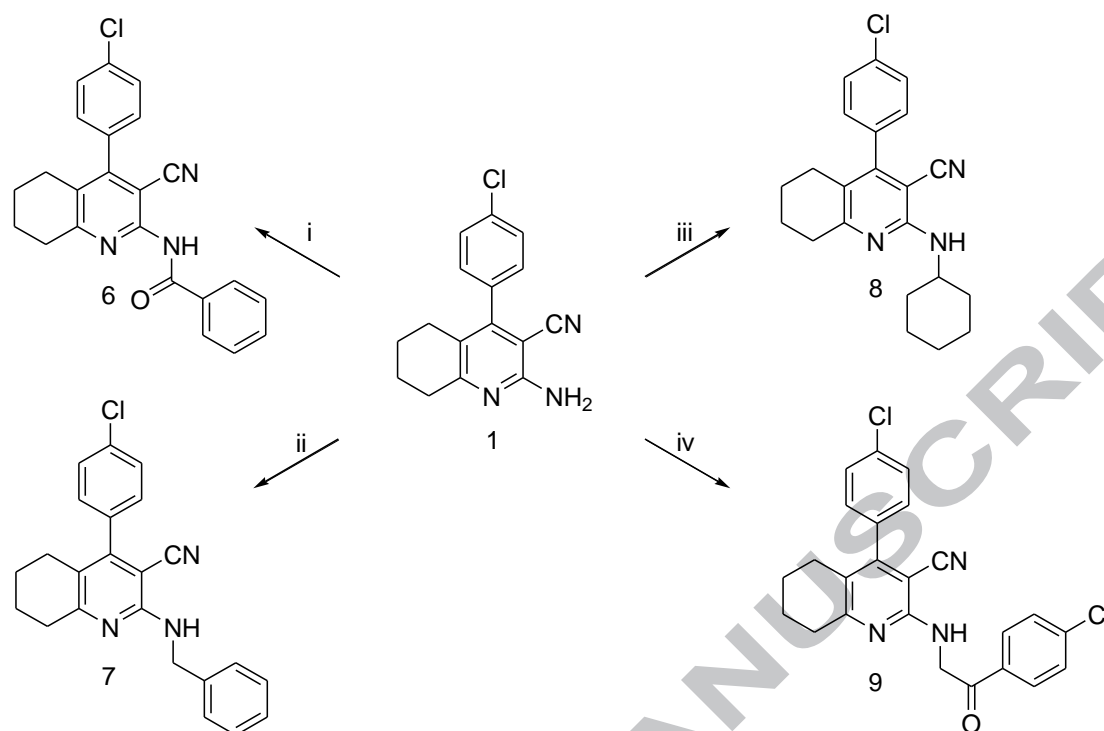


**Reagents and reaction conditions:** i: 70%  $\text{H}_2\text{SO}_4$ , heat over waterbath, 5h; ii:  $\text{R}^1\text{-C}_6\text{H}_4\text{-NCS}$ , pyridine, reflux, 10h; iii:  $\text{R}^2\text{-C}_6\text{H}_4\text{-CHO}$ , pyridine, reflux, 6h; iv:  $\text{C}_6\text{H}_5\text{-CONHNH}_2$ , fusion at  $180\text{-}200^\circ\text{C}$ , 1h.

Figure 4: Synthesis of the target compounds 2-5

Fig. 5 illustrates the synthesis of target compounds 6-9, where acylation of the amino group at the 2 position of compound 1 with benzoyl chloride yielded the amide 6 showing the expected absorption bands for newly formed amide functional group in its IR spectrum. The spectrum also retained the absorption band for the CN group. Its  $^{13}\text{C-NMR}$  retained the signal for the CN group at  $\delta = 115$  ppm in addition to the appearance of a new signal at  $\delta = 167$  ppm corresponding to the C=O.

While alkylation of compound 1 with different alkyl halides such as benzyl chloride, cyclohexyl bromide and phenacyl bromide yielded the designed alkylated amines 7-9.  $^{13}\text{C-NMR}$  of compound 9 retained the signal for the CN group at  $\delta = 115$  ppm in addition to the appearance of a new signal at  $\delta = 168$  ppm corresponding to the C=O.

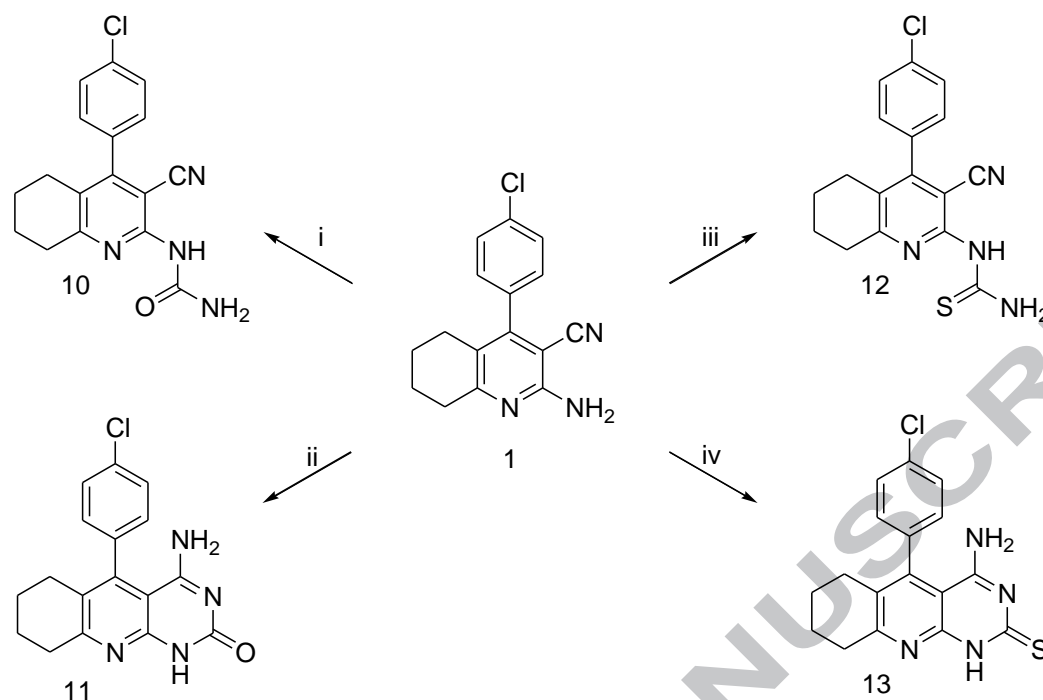


**Reagents and reaction conditions:** i:  $\text{C}_6\text{H}_5\text{COCl}$ , dioxan, reflux, 10h; ii:  $\text{C}_6\text{H}_5\text{CH}_2\text{Cl}$ , dioxan, reflux, 10h; iii:  $\text{C}_6\text{H}_{10}\text{Br}$ , dioxan, reflux, 5h; iv:  $\text{ClC}_6\text{H}_4\text{COCH}_2\text{Br}$ , dioxan, reflux, 6h.

Figure 5: Synthesis of the target compounds 6-9

Finally, in Fig. 6 fusion of compound **1** with urea and thiourea at different reaction temperatures resulted in different products. Using moderate temperatures in this reaction resulted in the open chain urea and thiourea derivatives (**10** and **12** respectively). This was proved by the presence of an absorption band characteristic for the cyano group at the 3-position in their IR spectra. Furthermore,  $^{13}\text{C}$ -NMR of both compounds retained the signal for the CN group at  $\delta = 116$  ppm in addition to the appearance of a new signal at  $\delta = 156$  and 185 ppm corresponding to the C=O and C=S respectively.

While utilizing higher temperatures for the same reaction resulted in cyclization of the side chain into the pyrimidinone and pyrimidinethione derivatives (**11** and **13** respectively) which has been verified by the disappearance of the nitrile absorption bands in their IR spectra. In addition, their  $^{13}\text{C}$ -NMR of compound **13** lacked the signal for the CN group and revealed the appearance of a new signal at  $\delta = 156$  and 182 ppm corresponding to the C=O and C=S respectively.



**Reagents and reaction conditions:** i: urea, fusion at 180-200°C, 1h; ii: urea, fusion at 280-300°C, 1h; iii: thiourea, fusion at 180-200°C, 1h; iv: thiourea, fusion at 280-300°C.

Figure 6: Synthesis of the target compounds 10-13

## 2.2. Biological evaluation

### 2.2.1. Acetylcholinesterase inhibitory activity

AChE is the enzyme responsible for the hydrolysis of ACh into acetyl CoA and choline thus terminating its effect at the cholinergic receptors. Accordingly, its inhibition would be expected to result in increasing the amount of ACh available for neural transmission at the receptor site and thus will most likely be successful in relieving some cognitive as well as behavioral symptoms of AD. Accordingly, all newly synthesized compounds were evaluated for their AChE inhibitory effect using both *in vitro* and *in vivo* pharmacological experiments.

#### 2.2.1.1. *In vitro* Acetylcholinesterase inhibitory activity

The *in-vitro* biological activities of the synthesized target compounds were evaluated through measuring the percentage increase in the contraction of frog's Rectus abdominis [39], a skeletal muscle that is known to be rich in AChE [40]. Such muscle contractions could be measured using force displacement transducer (FTO 3C) connected to a grass polyview 16 data acquisition and analysis system version 1 Grass technology WARWICK, RI, USA. Therefore, administration of an AChEI before the addition of ACh to a muscle preparation should result in accumulation of unhydrolyzed ACh with resultant increase in the height of ACh induced contractions. The difference in height of ACh induced contractions of the muscle before and after exposure to a suspected AChEI is considered as an indication of the extent of its inhibitory effect on the enzyme.

The percentage inhibition of AChE activity was determined. The values  $\pm$  standard deviation (at confidence levels of 95 %) are recorded in Table 1 and presented in Fig. 7. Tacrine was used as a reference standard.

**Table 1:** *In vitro* and *in vivo* AChE inhibitory activity, biochemical estimation of the liver enzymes; serum glutamic pyruvated transaminase (SGPT) and reduced glutathione (GSH) levels in liver homogenate level.

Compound	<i>In vitro</i> Increase in contraction (%) <sup>a</sup>	<i>In vivo</i> AChE activity % inhibition <sup>b</sup>	SGPT(IU/mL) <sup>c</sup>	GSH ( $\mu$ g/mL) <sup>c</sup>
Saline			47.25 $\pm$ 4.5	0.24 $\pm$ 0.027
Control	5.3 $\pm$ 1.7	0.00 $\pm$ 6.60	204.3 $\pm$ 26.5	0.15 $\pm$ 0.042
Tacrine	37.5 $\pm$ 3.5	9.0 $\pm$ 0.5	304.7 $\pm$ 30.9	0.12 $\pm$ 0.026
2	41.2 $\pm$ 4.5	15.8 $\pm$ 0.04	47.25 $\pm$ 4.5	0.16 $\pm$ 0.011
3a	28.9 $\pm$ 1.6	17.6 $\pm$ 1.2	158.08.5 $\pm$ 6.3	
3b	11.9 $\pm$ 1.3	22.7 $\pm$ 1.1	70.0 $\pm$ 8.5	0.19 $\pm$ 0.012
3c	34.2 $\pm$ 1.2	18.9 $\pm$ 1.5	176.75 $\pm$ 10.0	
4a	44.9 $\pm$ 7.7	16.3 $\pm$ 1.6	46.08 $\pm$ 25.7	0.21 $\pm$ 0.019
4b	36.01 $\pm$ 2.7	17.3 $\pm$ 1.3	74.66 $\pm$ 8.9	0.23 $\pm$ 0.012
5	13.96 $\pm$ 1.4	22.7 $\pm$ 1.6	196.0 $\pm$ 10.2	
6	21.6 $\pm$ 7.1	17.8 $\pm$ 1.9	191.0 $\pm$ 10.6	
7	71.3 $\pm$ 1.2	17.3 $\pm$ 0.6	146.41 $\pm$ 9.8	
8	46.8 $\pm$ 1.0	16.9 $\pm$ 1.2	127.75 $\pm$ 16.7	
9	48.7 $\pm$ 1.7	21.6 $\pm$ 1.4	141.16 $\pm$ 9.8	
10	48.9 $\pm$ 3.9	14.8 $\pm$ 1.3	106.16 $\pm$ 3.7	
11	48.3 $\pm$ 4.8	18.4 $\pm$ 1.3	187.25 $\pm$ 17.2	
12	50.6 $\pm$ 1.0	14.8 $\pm$ 1.3	167.41 $\pm$ 2.5	
13	29.1 $\pm$ 1.6	16.5 $\pm$ 1.2	201.25 $\pm$ 16.7	

<sup>a</sup>The tested compounds were added at a concentration of 1  $\mu$ mol.

<sup>b</sup>The tested compounds were added at a concentration of 1  $\mu$ mol /Kg body weight.

<sup>c</sup>The tested compounds were added at a concentration of 7 mg/Kg body weight.

Data are expressed as means $\pm$ SD (n=5) of at least three different experiments.

Data were analyzed using One factor ANOVA followed by *post hoc* Tukey simultaneous comparison t-values (pairwise t-tests).

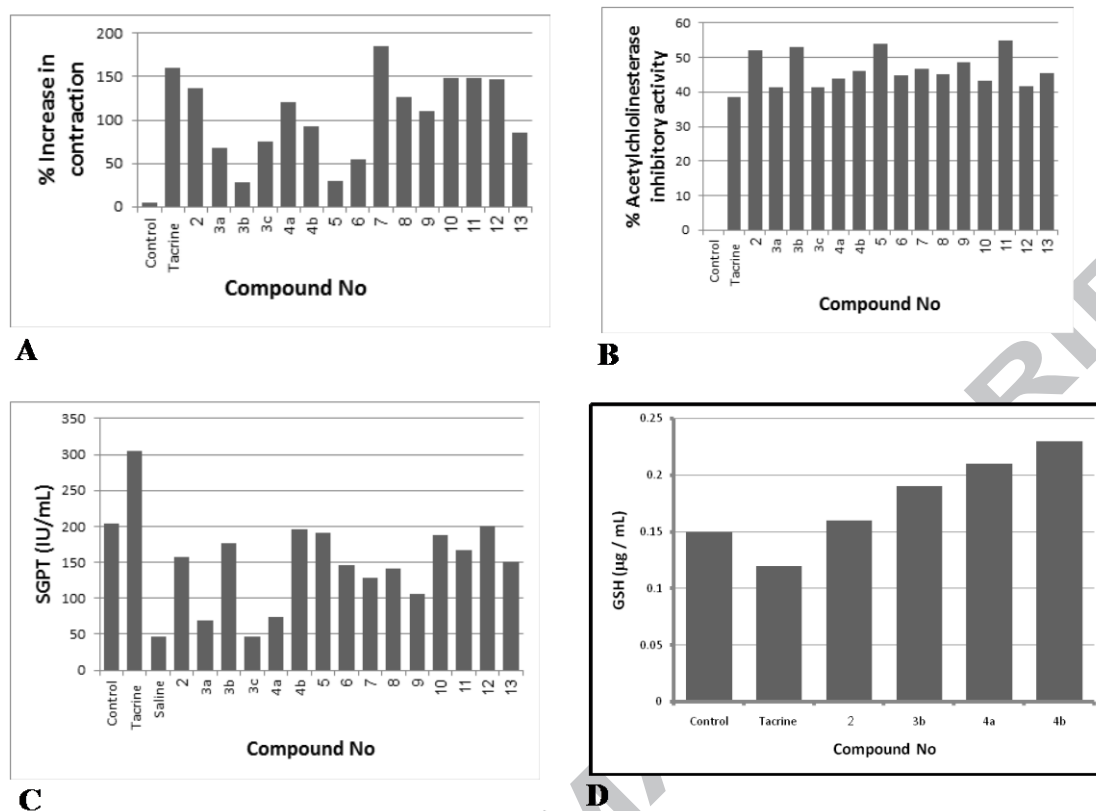


**Figure 7:** (A): *In vitro* percentage AChE inhibitory activity of the synthesized compounds at a dose 1  $\mu\text{mol}$ . Values are expressed as % increase in acetyl choline induced contraction in the isolated rectus abdominis. (B): *In vivo* percentage AChE inhibitory activity of the synthesized compounds at a dose 1  $\mu\text{mol/Kg}$  body weight. Values are expressed as % increase in AChE activity in rat brain using Ellman method. (C): SGPT levels of the synthesized compounds at a dose of 7mg/Kg body weight. (D): GSH levels of the selected compounds at a dose of 7mg/Kg body weight

Results, in general, revealed that all tested compounds except **3b**, **5** and **6** showed promising AChE inhibitory activities. Correlating these results with structures of the tested compounds indicated that nature of substituents at the 3-position of the pyridine ring doesn't affect biological activity. However, the type of substituents at the 2-position has a noticeable impact on activity where the presence of an amino group whether free (**2**) or substituted by an alkyl group (**4a,b** and **7-9**) resulted in equivalent or higher activity than tacrine (36% -71% *in vitro* increase in contraction relative to 37.5% in case of tacrine) with the 2-benzylamino substituent (**7**) showing the highest activity (71.3%). On the other hand, introduction of an amide group at the 2-position of the pyridine ring either through acylation of the amino group (**5**) or incorporation of an acylated hydrazine moiety (**6**) resulted in a noticeable reduction in the inhibitory activity. Nevertheless, if the amide group is a part of a urea (**10**) or thiourea (**12**) side chains, the products maintained high activity (almost 1.5 fold tacrine's activity). Furthermore, cyclization of the urea side chains into a pyrimidine nucleus (**11**) maintained the high activity while cyclization of the thiourea side chains (**3a-c** and **13**) either decreased or abolished the activity.

#### 2.2.1.2. *In vivo* acetyl cholinesterase inhibitory activity

All synthesized target compounds were further investigated by the quantitative *in-vivo* anti-cholinesterase assay according to the method developed by Ellman et al [41]. The principle of the assay relies on the fact that the active enzyme hydrolyzes acetyl thiocholine releasing free thiocholine which upon reaction with Ellman reagent [DTNB; 5,5'-dithiobis-(2-nitrobenzoic acid)]

will form a yellow colored disulfide complex. The intensity of the yellow color produced due to the amount of hydrolyzed thiocholine is therefore considered as a reliable measure of the activity of AChE. In other words, a decrease in the intensity of the yellow color is proportional to the amount of produced thiocholine relative to the control indicating a decrease in AChE activity and thus a successful anti-cholinesterase effect [42]. The results  $\pm$  standard deviation (at confidence levels of 95 %) are recorded in Table 1 and presented in Fig. 7. Tacrine was used as a reference standard.

The results revealed that all compounds showed high anti-cholinesterase activity with percentage inhibition ranging from 14.8% to 22.7% relative to 9% in case of tacrine. The fact that the *in vitro* inactive compounds (**3b**, **5** and **6**) showed promising *in vivo* AChE inhibitory activity indicates that they can be regarded as pro-drugs where they are metabolized in the body into active metabolites.

### 2.2.2. Hepatotoxicity testing

All newly synthesized compounds were evaluated for their hepatotoxicity through determination of their serum glutamic pyruvic transaminase (SGPT) levels. Compounds showing promising results were further investigated through determination of their reduced glutathione (GSH) levels in rat's liver.

#### 2.2.2.1. Alanine transaminase (ALT) "Serum glutamic pyruvated transaminase (SGPT)" assay

Since all target compounds showed either *in vitro* and/or *in vivo* anti-AChE inhibitory activity that was significantly different from control values at  $P < 0.05$ , thus hepatotoxicity of all compounds was tested through determination of SGPT levels using Ultraviolet (UV) kinetic method in which SGPT was assayed based on enzyme coupled system. SGPT is an enzyme that is involved in the transfer of an amino group from alanine to an  $\alpha$ -ketoacid (2-oxoglutarate) resulting into the formation of a pyruvate moiety. The formed pyruvate is reduced into L-lactate by NADH which is itself oxidized to NAD and the rate of oxidation is measured through determination of the absorbance at 340 nm at 0,1,2,3 minutes.

The higher the values obtained for SGPT, the higher the hepatotoxicity caused and vice versa [43, 44]. The results  $\pm$  standard deviation (at confidence levels of 95 %) are recorded in Table 1 and presented in Fig. 7.

The results indicated that dimethyl formamide (DMF, the solvent used) showed considerably high hepatotoxicity itself thus SGPT levels for saline were calculated to determine its normal levels. All the synthesized compounds, unlike tacrine, lacked any hepatotoxic effect (SGPT levels ranging from 46 to 201 IU/mL relative to 304 IU/mL in case of tacrine and 204 IU/mL for the control). Compounds containing the amide linkage in the open chain substituent at the 2-position (**5**, **6**) didn't show any hepatotoxicity and maintained SGPT levels similar to that of the control. However, if the amide group is a part of a urea (**10**) or thiourea (**12**) side chains, the products were capable of reducing the hepatotoxic effect of the solvent (106 and 167 IU/mL). On the other hand, cyclization of the urea or thiourea side chains into a pyrimidine nucleus (**11**, **13**) resulted in compounds that didn't show any hepatotoxicity but were incapable of reducing the hepatotoxicity of the solvent showing SGPT levels almost the same as DMF. Nevertheless,

arylation of the N<sup>3</sup> of the fused pyrimidine ring slightly improved the hepatoprotective effect of the synthesized compounds against the solvent used. To conclude, all compounds except **5**, **6**, **11** and **13** were capable of reducing the hepatotoxic effect of the solvent used DMF. In addition, compounds **2**, **3a**, **4a** and **4b** almost brought SGPT levels back to its normal values (saline values) despite the presence of DMF. In other words, the compounds not only lacked a hepatotoxic effect, they were to some extent hepatoprotective against the effect of the solvent used.

#### 2.2.2.2. Reduced glutathione (GSH) assay

Furthermore, reduced GSH in rats' livers was evaluated for the four compounds that showed a somewhat hepatoprotective effect against the solvent's toxicity and brought SGPT levels to its normal saline values (**2**, **3b**, **4a** and **4b**). The major objective was to investigate the effect of GSH depletion and oxidative stress on the toxicity induced by tacrine and selected compounds in liver homogenate. Reduced GSH as a major antioxidant in hepatocytes acts as a scavenger that can protect hepatocytes against oxidative stress through its ability to conjugate to a variety of electrophiles leading to their detoxication [45]. The balance of glutathione redox cycle is an important mechanism for cell protection. Literature survey indicated that depletion of cellular GSH has been demonstrated in the toxicity associated with tacrine. The production of the undesired protein reactive metabolites was significantly reduced by GSH. Reduced levels of cellular GSH resulted in pathophysiological formation of reactive oxygen species and cellular damage occurred [46].

The lower the values obtained for reduced GSH, the higher the hepatotoxicity caused and vice versa. Tacrine was found to cause reduction in GSH levels in rats' liver. This observation was consistent with other studies that reported the reduction of hepatic GSH level in rats given tacrine [47].

The results  $\pm$  standard deviation (at confidence levels of 95 %) are recorded in Table 1 and presented in Fig. 7.

The results again indicated that DMF showed considerably high hepatotoxicity itself thus GSH levels for saline were calculated to determine its normal levels. Tacrine caused further reduction of GSH levels indicating higher hepatotoxicity than DMF. All the tested compounds, unlike tacrine, lacked any hepatotoxic effect with GSH levels ranging from 0.16 to 0.23  $\mu\text{g}/\text{mL}$  relative to 0.15  $\mu\text{g}/\text{mL}$  in case of DMF and 0.12  $\mu\text{g}/\text{mL}$  for the standard drug used (tacrine). Compounds **4b** almost brought GSH level back to its normal values (0.23  $\mu\text{g}/\text{mL}$  reduced GSH relative to a value of 0.24  $\mu\text{g}/\text{mL}$  in case of saline) despite the presence of DMF.

### 2.3. Physicochemical properties and pharmacokinetic parameters determination.

#### 2.3.1. Theoretical *in silico* prediction of physicochemical properties and pharmacokinetic parameters.

Research over the last few decades indicated that compounds having good pharmacological activities may fail to become good drug candidates due to low bioavailability [48]. Thus physicochemical properties and pharmacokinetic parameters of newly synthesized compounds are criteria that have to be carefully considered in the drug discovery and development processes. Absorption, distribution, metabolism and excretion (ADME) of a drug candidate are

crucial for successful *in vivo* therapeutic activity [49]. These properties can be predicted using computer software. *In silico* ADME computational studies are used nowadays to select the most promising compound and thus reduce costly late stage failures in drug development processes [50]. Through virtual ADMET screening software [36], the different physicochemical properties of the newly synthesized compounds were calculated such as partition coefficient (logP), solubility (S) and topological polar surface area (TPSA). Furthermore, pharmacokinetic parameters such as percentage of human intestinal absorption (HIA), plasma protein binding (PPB), as well as blood brain barrier penetration (BBB) were determined using the preADMET software [35]. Finally, a collective numerical representation of physicochemical properties, pharmacokinetics and pharmacodynamics for each compound was thus computed and expressed as drug likeness score [34].

All computed descriptors were listed in Table 2.

**Table 2:** *In silico* physicochemical and pharmacokinetic parameters.

Comp. No.	logP <sup>a</sup>	Practical logP <sup>b</sup>	S <sup>c</sup>	TPSA <sup>d</sup>	HIA <sup>e</sup>	BBB <sup>f</sup>	PPB <sup>g</sup>	Lipinski's violation (theoretical)	Lipinski's violation (practical)	Drug-likeness model score
2	3.09	3.099	1.83	82.01	94.77	0.80	100	0	0	1.06
3a	4.11	4.900	2.4*10 <sup>-4</sup>	57.47	93.75	8.34	90.81	0	0	0.86
3b	4.56	3.570	7.1*10 <sup>-5</sup>	57.47	93.84	8.95	88.89	0	0	0.53
3c	4.79	4.837	3.4*10 <sup>-5</sup>	57.47	94.14	9.14	94.95	0	0	0.45
4a	6.07	4.866	8.9*10 <sup>-3</sup>	49.05	97.66	0.50	100	1	0	0.56
4b	6.01	4.807	1.7*10 <sup>-2</sup>	69.28	96.58	0.67	100	1	0	0.87
5	5.19	4.400	1.9*10 <sup>-2</sup>	77.81	95.43	2.69	100	1	0	1.14
6	5.43	2.972	1.2*10 <sup>-2</sup>	65.78	96.61	0.51	98.19	1	0	1.31
7	5.79	3.750	5.99*10 <sup>-3</sup>	48.71	96.78	3.68	100	1	0	1.09
8	6.30	2.435	7.9*10 <sup>-3</sup>	48.71	96.42	6.83	100	1	0	0.76
9	6.22	4.814	2.3*10 <sup>-4</sup>	65.78	97.13	1.24	100	1	0	0.92
10	3.67	4.438	3.1*10 <sup>-1</sup>	91.81	94.52	0.17	89.84	0	0	1.73
11	3.68	4.686	1.1*10 <sup>-1</sup>	84.67	94.58	0.38	96.84	0	0	1.37
12	4.21	4.026	2.2*10 <sup>-2</sup>	74.73	95.63	0.46	100	0	0	1.45
13	4.03	4.685	1.6*10 <sup>-2</sup>	67.60	95.66	0.65	100	0	0	1.08

<sup>a</sup>LogP: logarithm of compound partition coefficient between n-octanol and water.

<sup>b</sup>Data are expressed as means of at least three different experiments.

<sup>c</sup>S: solubility.

<sup>d</sup>TPSA: topological polar surface area.

<sup>e</sup>HIA: percentage human intestinal absorption.

<sup>f</sup>BBB: blood brain barrier penetration is the ratio of steady state concentration in brain to those in blood.

<sup>g</sup>PPB: plasma protein binding.

From the previous calculations, eight compounds obeyed Lipinski's rule of five [51] which is considered as an important parameter to select drug-like candidates. Where logP values represent the ratio of concentration of a compound in two immiscible phases at equilibrium thus it is a measure of drug affinity towards lipophilic bilayer plasma membranes. Large logP values reflect higher level of lipophilicity. Other parameters such as topological polar surface area (TPSA) and solubility are regarded as vital descriptors for oral bioavailability and blood brain barrier (BBB) penetration, where high solubility is considered as a prerequisite for a rapid absorption and higher bioavailability of a drug candidate. As for TPSA, it is regarded as a critical parameter for human intestinal absorption, cell permeability and blood brain barrier (BBB) penetration. Results indicated that all synthesized compounds showed TPSA values less than 140

$\text{\AA}^2$  indicating good permeability through intestine, which was further proven by their HIA values which were all above 90%. Furthermore, the TPSA values for all synthesized compounds, except compound **10**, were less than  $90 \text{ \AA}^2$  implying reasonable BBB penetration which was further proven by their BBB values where all compounds showed values above 0.1. Compounds **3a-c**, **5**, **7** and **8** showed BBB values higher than 2 indicating high CNS absorption. Compounds **3a-c** and **8** exhibited outstanding BBB penetration values (6.83-9.14) indicating their stupendous CNS absorption.

It is worth mentioning that some researchers [52, 53] have limited CNS drugs activity to compounds having logP in the range 2-4, however, they eventually concluded that this is just a preferred range and that it remains acceptable for CNS drugs to have logP values in the range 2-5. This was highly consistent with the results obtained in the present study, where all the synthesized compounds showed *in vivo* ACHE inhibitory activities (even the compounds that were inactive *in vitro*) despite the fact that their logP values of most of them were higher than 4.

Screening plasma protein binding revealed that all investigated compounds were strongly bound to plasma proteins except compounds **3b** and **10** which were moderately bound to plasma proteins (88.89 and 89.94% respectively). Nine compounds (**2**, **4a,b**, **5**, **7-9**, **12**, **13**) out of the fifteen synthesized compounds showed 100% plasma protein binding capabilities. However, all Lipinski's violations were due to logP values more than 5. In conclusion, the majority of the synthesized compounds showed reasonable to high pharmacokinetic properties. Finally, the drug-likeness score of the synthesized compound was predicted, the higher the value of the score is, the higher the probability that the particular molecule will be regarded as drug-like candidate. Results revealed that all synthesized compounds possessed a positive drug-like score value and thus considered as drug-like. Furthermore, Eight out of the synthesized compounds (**2**, **5-7**, **10-13**) showed drug-likeness values above 1. Other important issues, such as compliance with Lipinski's rule of five, acceptable HIA, PPB and BBB penetration advocated these compounds to be drug-like candidates.

### 2.3.2. Experimental determination of LogP.

Theoretical calculations indicated that seven out of the fifteen synthesized compounds showed logP values higher than 5 and thus violating Lipinski's rule of five. However, these results were not consistent with the fact that all synthesized compounds showed high *in vivo* anti-cholinesterase activities. Accordingly, practical logP testing was performed. Determination of the partition coefficient (LogP) was accomplished using capacity factor calculation method, as previously described [54]. Reverse Phase High Performance Liquid Chromatography (RP-HPLC) was used for the determination. In brief, the octanol/water partition coefficient of the synthesized compounds was determined from the qualitative analysis of its capacity factor 'k' which was calculated through determination of retention time and dead time (the average time needed by a solvent molecule to pass the column) [55]. Four reference standards, benzoic acid, toluene, anthraquinone and benzyl benzoate, which are structurally related to the compounds being tested, were selected to cover LogP range from 1.9 to 4. The results are recorded in Table 2. Capacity factor (k) for each compound was determined using the following equation:

$$k = \frac{t_R - t_0}{t_0}$$

Where k is the capacity factor,  $t_R$  is the retention time of the test compound, and  $t_0$  is the dead-time. Unretained thiourea was used to measure the dead time  $t_0$ . The results indicated that all

compounds had logP values less than 5 and thus are promising hits and /or leads as anti-cholinesterase inhibitors.

## 2.4. Docking studies

Docking study was carried out using the enzyme parameters obtained from the crystallographic structure of the complex between AChE (PDB ID: 6g1u) with the co-crystallized ligand tacrine derivative 6-chloroanyl-10-methyl-1,2,3,4-tetrahydroacridin-10-ium-9-amine [56]. The docking simulation for the ligand (tacrine) was carried out using molecular operating environment (MOE) software supplied by the Chemical Computing Group, Inc., Montréal, QC [44] (Fig. 8A). The X-ray crystal structure revealed that the NH group in the ligand tacrine is hydrogen-bonded to His 480, while the phenyl ring displayed arene-arene interactions with Trp 83 and Tyr 370 residues. Besides, it showed hydrophobic interactions with Trp 83, Gly 149, Gly 150, Tyr 162, Glu 237, Tyr 370 and His 480. Figure 8B shows the binding mode of compounds **7** indicating a superior binding score (-3.3252) relative to the ligand used (tacrine -2.7680). Furthermore, a hydrogen bond is observed between the side chain NH and ASP93 and another hydrogen bond is present between the nitrogen of the CN group and Tyr96. In addition, compound **7** displayed hydrophobic interactions with Leu31, Gly32, Trp58, Asn59, Thr63, Pro64, Asn65 and Ser91.

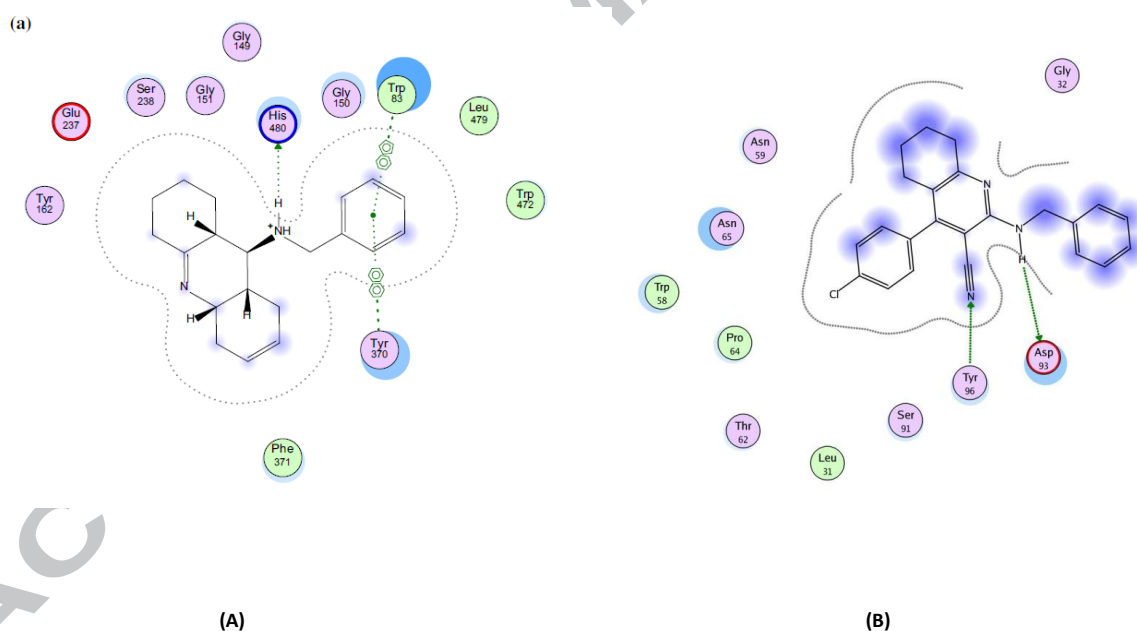


**Figure 8:** (A) Binding mode of the inhibitor (tacrine) in the binding site of *hAChE* (PDB ID: 6g1u) using MOE software and (B) Binding mode of compound **7** docked and minimized in the binding site of *hAChE* (PDB ID: 6g1u) using MOE software

## 3. Conclusion

Due to the hepatotoxicity associated with the use of tacrine as AChEI in the treatment of AD, this study portrays the synthesis of fifteen chlorinated tetrahydroquinolines to serve as tacrine analogs with lower hepatotoxicity. The *in vitro* testing of the synthesized compounds as AChEIs revealed that the 2-benzylamino derivative (**7**) showed twice the inhibitory activity of tacrine. Other 2-alkylamino compounds showed cholinesterase inhibitory activities comparable to or slightly higher than tacrine. However, results revealed that incorporation of an amide bond in the

side chain at the 2-position is not preferable except if it is a part of a urea or thiourea side chains. Fusion of the pyridine ring to a pyrimidine nucleus was regarded in most cases unsuccessful in producing promising AChEIs. The *in vivo* screening of the synthesized compounds as AChEIs revealed that all compounds showed inhibitory effect equivalent to or significantly higher (2.5 fold) than tacrine with compounds **3b**, **5** and **9** showing the highest *in vivo* percentage inhibition (>20% AChE inhibition compared to 9% in case of tacrine). It could be concluded that hydrolysis of the amide bond and opening of the fused pyrimidine ring takes place during metabolism *in vivo* resulting in retaining the abolished activity of some products (**3b** and **5**). In addition, hepatotoxicity screening of the compounds was estimated by determination of levels of SGPT and reduced GSH. SGPT testing indicated that all compounds were safe to the liver with ten compounds possessing hepatoprotective effect against the toxic effect of the solvent used (DMF). Furthermore, four compounds; **2**, **3b**, **4a** and **4b** were able to completely reverse the effect of the solvent and result in SGPT values almost similar to that of saline. Finally, the four most promising compounds that brought SGPT values back to normal were further investigated through determination of reduced GSH levels in rat liver after administration of the tested compounds. The results indicated that these compounds showed no hepatic injury and less GSH depletion than tacrine. Therefore, the hypothesis that the presence of a chloro group in tacrine related analogs results in encouraging anti-cholinesterase activity and most importantly reduced hepatotoxicity deserves further investigation. Furthermore, *in silico* physicochemical properties and pharmacokinetic parameters for the synthesized compounds were calculated using computer software and their practical logP determined. In addition, their drug-likeness score was calculated. Results indicated that all drugs are promising drug-like candidates. Finally, docking simulation of the *in vitro* most active compound **7** indicated superior binding to the receptor over tacrine.

## 4. Experimental

### 4.1. Chemistry

All reagents and solvents were purchased from commercial suppliers and were dried and purified when necessary by standard techniques. Melting points were determined in open glass capillaries using Thomas-Hoover melting point apparatus. Infrared spectra (IR) were recorded, using KBr discs, by a Perkin-Elmer 1430 Infrared spectrophotometer. Nuclear magnetic resonance ( $^1\text{H-NMR}$  and  $^{13}\text{C-NMR}$ ) were determined using a Bruker 300 ultrashield spectrophotometer. The data were reported as chemical shifts or  $\delta$  values (ppm) relative to tetramethylsilane (TMS) as internal standard. Elemental microanalyses were performed at the regional center for Mycology and Biotechnology, Al-Azhar University and the values were within  $\pm 0.4\%$  of the theoretical values. Reaction progress was monitored by thin-layer chromatography (TLC) on silica gel sheets (60 GF254, Merck). The spots were visualized by exposure to iodine vapor or UV-lamp at  $\lambda$  254 nm for few seconds.

Compounds **1**, **2** and **7** were prepared according to reported procedures [5, 37, 38, 57, 58].

#### 4.1.1. General procedure for the preparation of 5-(4-chlorophenyl)-3,4,6,7,8,9-hexahydro-4-imino-3-arylpyrimido[4,5-b]quinoline-2(1H)-thione (**3a-c**)

A mixture of **1** (1 mmol; 0.28 g) and the appropriate isothiocyanate (1 mmol) in pyridine (10 ml) was heated under reflux for 10 h. The reaction mixture was cooled then poured onto ice-water.

The obtained solid was filtered, washed several times with water, dried and recrystallized from acetic acid. IR (KBr,  $\text{cm}^{-1}$ ): 3327-3180 (NH), 1210 (C=S).

**4.1.1.1. 5-(4-chlorophenyl)-3,4,6,7,8,9-hexahydro-4-imino-3-phenylpyrimido[4,5-b]quinoline-2(1H)-thione (3a)**

Brownish yellow crystals (0.36 g, 86%); m.p. 134-136 $^{\circ}\text{C}$ .  $^1\text{H-NMR}$  (300 MHz,  $\text{CDCl}_3$ ):  $\delta$  1.57-1.61 (m, 2H,  $\text{C}_6\text{-H}_2$ ), 1.71-1.76 (m, 2H,  $\text{C}_7\text{-H}_2$ ), 2.38-2.45 (t,  $J = 8.7$  Hz, 2H,  $\text{C}_5\text{-H}_2$ ), 2.87-2.93 (t,  $J = 8.7$  Hz, 2H,  $\text{C}_8\text{H}_2$ ), 7.001-7.47 (m, 10H, Ar-H and NH) and 11.77 (s, 1H, NH,  $\text{D}_2\text{O}$ -exchangeable);  $^{13}\text{C-NMR}$  (75 MHz,  $[\text{D}_6]\text{DMSO}$ ):  $\delta$  22.8, 26.3, 32.4, 33.3 (cyclohexyl-C), 117, 125, 127, 127.7, 128.6, 129, 129.5, 135, 138, 154, 157, 162 (Ar-C), 167.5 (C=NH) and 180 (C=S); Anal. calcd. For  $\text{C}_{23}\text{H}_{19}\text{ClN}_4\text{S}$  (418.94): C, 65.94; H, 4.57; N, 13.37. Found: C, 65.67; H, 4.81; N, 13.45.

**4.1.1.2. 5-(4-chlorophenyl)-3,4,6,7,8,9-hexahydro-4-imino-3-*p*-tolylpyrimido[4,5-b]quinoline-2(1H)-thione (3b)**

Brownish yellow crystals (0.37 g, 85%); m.p. 146-148 $^{\circ}\text{C}$ .  $^1\text{H-NMR}$  (300 MHz,  $[\text{D}_6]\text{DMSO}$ ):  $\delta$  1.58-1.80 (m, 4H,  $\text{C}_6\text{-H}_2$  and  $\text{C}_7\text{-H}_2$ ), 2.39-2.40 (dist. t, 5H,  $\text{C}_5\text{-H}_2$  and  $\text{CH}_3$ ), 2.75-2.78 (dist. t, 2H,  $\text{C}_8\text{-H}_2$ ), 7.44-7.61 (m, 8H, Ar-H), 10.56 (s, 1H, NH,  $\text{D}_2\text{O}$ -exchangeable) and 11.22 (s, 1H, NH,  $\text{D}_2\text{O}$ -exchangeable);  $^{13}\text{C-NMR}$  (75 MHz,  $[\text{D}_6]\text{DMSO}$ ):  $\delta$  22, 24.8, 26.5, 32.4, 33.5 (cyclohexyl-C and 4-Ph- $\text{CH}_3$ ), 117, 127, 128, 128.5, 129, 129.8, 132, 135, 138, 153.9, 157.2, 161.8 (Ar-C), 167.3 (C=NH) and 181.4 (C=S); Anal. calcd. for  $\text{C}_{24}\text{H}_{21}\text{ClN}_4\text{S}$  (432.97): C, 66.58; H, 4.89; N, 12.94. Found: C, 66.65; H, 4.99; N, 12.81.

**4.1.1.3. 3,5-bis(4-chlorophenyl)-3,4,6,7,8,9-hexahydro-4-iminopyrimido[4,5-b]quinoline-2(1H)-thione (3c)**

Yellow crystals (0.39 g, 86%); m.p. 120-122 $^{\circ}\text{C}$ .  $^1\text{H-NMR}$  (300 MHz,  $[\text{D}_6]\text{DMSO}$ ):  $\delta$  1.70-1.73 (m, 2H,  $\text{C}_6\text{-H}_2$ ), 1.84-1.87 (m, 2H,  $\text{C}_7\text{-H}_2$ ), 2.51-2.53 (t,  $J = 4.5$  Hz, 2H,  $\text{C}_5\text{-H}_2$ ), 2.55-2.58 (t,  $J = 4.5$  Hz, 2H,  $\text{C}_8\text{-H}_2$ ), 7.00-7.47 (m, 8H, Ar-H), 8.49 (s, 1H, NH,  $\text{D}_2\text{O}$ -exchangeable) and 10.13 (s, 1H, NH,  $\text{D}_2\text{O}$ -exchangeable);  $^{13}\text{C-NMR}$  (75 MHz,  $[\text{D}_6]\text{DMSO}$ ):  $\delta$  22.1, 26.4, 32.5, 33.1 (cyclohexyl-C), 117.6, 127, 127.9, 128.3, 129, 129.4, 132, 135, 138, 153.9, 157.2, 161.9 (Ar-C), 167.4 (C=NH) and 181 (C=S); Anal. calcd. for  $\text{C}_{23}\text{H}_{18}\text{Cl}_2\text{N}_4\text{S}$  (453.39): C, 60.93; H, 4.00; N, 12.36. Found: C, 60.75; H, 4.21; N, 12.56.

**4.1.2. General procedure for the preparation of 2-(arylideneamino)-4-(4-chlorophenyl)-5,6,7,8-tetrahydroquinoline-3-carbonitrile (4a,b)**

A mixture of **1** (1 mmol; 0.28 g) and the appropriate aromatic aldehyde (1 mmol) in pyridine (10 ml) was heated under reflux for 6 h. The reaction mixture was cooled then poured onto ice-water. The obtained solid was filtered, washed several times with water, dried and recrystallized from dimethylformamide/water.

**4.1.2.1. 2-(benzylideneamino)-4-(4-chlorophenyl)-5,6,7,8-tetrahydroquinoline-3-carbonitrile (4a)**

Yellow crystals (0.33 g, 90%); m.p. 116-118 $^{\circ}\text{C}$ .  $^1\text{H-NMR}$  (300 MHz,  $\text{CDCl}_3$ ):  $\delta$  1.79-1.82 (m, 2H,  $\text{C}_6\text{-H}_2$ ), 1.96-1.98 (m, 2H,  $\text{C}_7\text{-H}_2$ ), 2.66-2.69 (t,  $J = 4.5$  Hz, 2H,  $\text{C}_5\text{-H}_2$ ), 3.22-3.28 (t,  $J = 4.5$  Hz, 2H,  $\text{C}_8\text{-H}_2$ ),

7.26-7.45 (m, 9H, Ar-H) and 8.7 (s, 1H, N = CH); <sup>13</sup>C-NMR (75 MHz, CDCl<sub>3</sub>): δ 25.37, 26.29, 27.32, 28.22 (cyclohexyl-C), 124.1 (CN), 128.66, 129.45, 130.6, 131.53, 132.9, 136.8, 137.3, 140.17, 145.7, 148.2, 154.4 (Ar-C); IR (KBr, cm<sup>-1</sup>): 2237 (CN); Anal. calcd. for C<sub>23</sub>H<sub>18</sub>ClN<sub>3</sub> (371.86): C, 74.29; H, 4.88; N, 11.30; Found: C, 74.15; H, 4.69; N, 11.23.

#### 4.1.2.2. 2-(2-hydroxybenzylideneamino)-4-(4-chlorophenyl)-5,6,7,8-tetrahydroquinoline-3-carbonitrile (4b)

Yellow crystals (0.34 g, 87%); m.p. 136-138<sup>o</sup>C. <sup>1</sup>H-NMR (300 MHz, [D<sub>6</sub>]DMSO): δ 1.73-1.74 (m, 2H, C<sub>6</sub>-H<sub>2</sub>), 1.9-1.93 (m, 2H, C<sub>7</sub>-H<sub>2</sub>), 2.58-2.61 (t, *J* = 4.5 Hz, 2H, C<sub>5</sub>-H<sub>2</sub>), 3.67-3.69 (dist t, 2H, C<sub>8</sub>-H<sub>2</sub>), 7.30-7.48 (m, 8 H, Ar-H), 8.66 (s, 1H, N = CH) and 10.02 (s, 1H, OH, D<sub>2</sub>O-exchangeable); <sup>13</sup>C-NMR (75 MHz, CDCl<sub>3</sub>): δ 23.57, 26.59, 27.92, 28.22 (cyclohexyl-C), 124.5 (CN), 114, 119, 129.45, 131.53, 136.8, 137.3, 140.17, 145.7, 148.2, 154.4, 161 (Ar-C); IR (KBr, cm<sup>-1</sup>): 3565 (OH), 2220 (CN); Anal. calcd. for C<sub>23</sub>H<sub>18</sub>ClN<sub>3</sub>O (387.86): C, 71.22; H, 4.68; N, 10.83. Found: C, 71.11; H, 4.53; N, 10.65.

#### 4.1.3. N'-(-4-(4-chlorophenyl)-3-cyano-5,6,7,8-tetrahydroquinolin-2-yl)benzohydrazide (5)

A mixture of **1** (1 mmol; 0.28 g) and benzoic acid hydrazide (1 mmol; 0.136 g) was fused at 280-281<sup>o</sup>C using a sand bath for 1 h. The reaction mixture was cooled then triturated with ethanol. The obtained solid was filtered, washed several times with water, dried and recrystallized from dimethylformamide/water. Brownish crystals (0.34 g, 84%); m.p. 181-183<sup>o</sup>C. <sup>1</sup>H-NMR (300 MHz, [D<sub>6</sub>]DMSO): δ 1.66-1.69 (m, 2H, C<sub>6</sub>-H<sub>2</sub>), 1.84-1.87 (m, 2H, C<sub>7</sub>-H<sub>2</sub>), 2.51-2.54 (dist. t, 2H, C<sub>5</sub>-H<sub>2</sub>), 3.64-3.65 (dist. t, 2H, C<sub>8</sub>-H<sub>2</sub>), 7.26-7.52 (m, 9H, Ar-H), 10.13 (s, 1H, NH, D<sub>2</sub>O-exchangeable) and 13.24 (s, 1H, NH, D<sub>2</sub>O-exchangeable); <sup>13</sup>C-NMR (75 MHz, [D<sub>6</sub>]DMSO): δ , 21.9, 26.4, 31.9, 32.6 (cyclohexyl-C), 115 (CN), 124.6, 128.6, 128.4, 129.2, 129.5, 133.4, 135.1, 139.4, 140.1, 153.5, 156.2, 159.7 (Ar-C) and 165.4 (C=O); IR (KBr, cm<sup>-1</sup>): 3561-3250 (NH), 2229 (CN), 1644 (C = O); Anal. calcd. for C<sub>23</sub>H<sub>19</sub>ClN<sub>4</sub>O (402.88): C, 68.57; H, 4.75; N, 13.91. Found: C, 68.29; H, 4.53; N, 13.65.

#### 4.1.4. N-(-4-(4-chlorophenyl)-3-cyano-5,6,7,8-tetrahydroquinolin-2-yl)benzamide (6)

A mixture of **1** (1 mmol; 0.28 g) and benzoyl chloride (1 mmol; 0.14 g) in dioxan(10 ml) was heated under reflux for 10 h. The reaction mixture was cooled then poured onto ice-water. The obtained solid was filtered, washed several times with water, dried and recrystallized from dimethylformamide/water. Yellowish white crystals (0.34 g, 88%); m.p. 271-272<sup>o</sup>C. <sup>1</sup>H-NMR (300 MHz, [D<sub>6</sub>]DMSO): δ 1.69-1.70 (m, 2H, C<sub>6</sub>-H<sub>2</sub>), 1.85-1.87 (m, 2H, C<sub>7</sub>-H<sub>2</sub>), 2.42-2.43 (dist. t, 2H, C<sub>5</sub>-H<sub>2</sub>), 3.01-3.03 (dist. t, 2H, C<sub>8</sub>-H<sub>2</sub>), 7.05-7.42 (m, 9H, Ar-H), and 12.778 (s, 1H, NH, D<sub>2</sub>O-exchangeable); <sup>13</sup>C-NMR (75 MHz, [D<sub>6</sub>]DMSO): δ , 21.8, 26.4, 31.7, 32.8 (cyclohexyl-C), 115.4 (CN), 124.7, 128.0, 128.3, 129.0, 129.2, 133.0, 135.1, 139.4, 140.2, 153.7, 156.2, 161.7 (Ar-C) and 167.4 (C=O); IR (KBr, cm<sup>-1</sup>): 3565-3230 (NH), 2239 (CN), 1654 (C = O); Anal. calcd. for C<sub>23</sub>H<sub>18</sub>ClN<sub>3</sub>O (387.86): C, 71.22; H, 4.68; N, 10.83. Found: C, 71.15; H, 4.43; N, 10.76.

#### 4.1.5. General procedure for the preparation of 2-(3alkylamino)-4-(4-chlorophenyl)-5,6,7,8-tetrahydroquinoline-3-carbonitrile (8,9)

A mixture of **1** (1 mmol; 0.28 g) and the appropriate alkyl halide (1 mmol) in dioxin (10 ml) was heated under reflux for 5-10 h. The reaction mixture was cooled then poured onto ice-water. The obtained solid was filtered, washed several times with water, dried and recrystallized from dimethylformamide/water.

#### 4.1.5.1. 4-(4-chlorophenyl)-2-(cyclohexylamino)-5,6,7,8-tetrahydroquinoline-3-carbonitrile (**8**)

Brown crystals (0.25 g, 69%); m.p. 160-162°C. <sup>1</sup>H-NMR (300 MHz, [D<sub>6</sub>]DMSO): δ 1.711-1.895 (m, 4H, C<sub>6</sub>-H<sub>2</sub> and C<sub>7</sub>-H<sub>2</sub>), 2.4044 (dist. t, 2H, C<sub>5</sub>-H<sub>2</sub>), 2.50.2.54 (dist. t, 2H; N-cyclohexyl-C<sub>4</sub>-H<sub>2</sub>), 2.56-2.68 (dist. t, 2H, C<sub>8</sub>-H<sub>2</sub>), 2.9874 (dist. t, 4H, N-cyclohexyl-C<sub>3</sub>-H<sub>2</sub> and C<sub>5</sub>-H<sub>2</sub>), 3.62-3.63 (dist. t, 4H, N-cyclohexyl-C<sub>2</sub>-H<sub>2</sub> and C<sub>6</sub>-H<sub>2</sub>), and 7.41-7.60 (m, 5H, Ar-H); <sup>13</sup>C-NMR (75 MHz, [D<sub>6</sub>]DMSO): δ 18.5, 24.1, 24.3, 30.6, 31.9, 45.5, 46.1, 51.8 (cyclohexyl-C), 113.8 (CN), 124.7, 127.9, 130.5, 131.3, 136.2, 157.2, 161.8, 167.2 (Ar-C); IR (KBr, cm<sup>-1</sup>): 2237 (CN); Anal. calcd. for C<sub>22</sub>H<sub>24</sub>ClN<sub>3</sub> (365.90): C, 72.22; H, 6.61; N, 11.48. Found: C, 72.34; H, 6.45; N, 11.41.

#### 4.1.5.2. 2-(4-(4-chlorophenyl)-3-cyano-5,6,7,8-tetrahydroquinolin-2-yl)amino-1-(4-chlorophenyl)ethanone (**9**)

Yellow crystals (0.39 g, 89%); m.p. 172-174°C. <sup>1</sup>H-NMR (300 MHz, [D<sub>6</sub>]DMSO): δ 1.67-1.72 (m, 2H, C<sub>6</sub>-H<sub>2</sub>), 1.80-1.83 (m, 2H, C<sub>7</sub>-H<sub>2</sub>), 2.44-2.50 (t, *J* = 9 Hz, 2H, C<sub>5</sub>-H<sub>2</sub>), 2.91-2.96 (t, *J* = 9 Hz, 2H, C<sub>8</sub>-H<sub>2</sub>), 4.0192 (s, 2H, N-CH<sub>2</sub>), 7.33-7.56 (m, 8H, Ar-H), and 11.8 (s, 1H, NH, D<sub>2</sub>O-exchangeable); <sup>13</sup>C-NMR (75 MHz, [D<sub>6</sub>]DMSO): δ 24.1, 26.4, 32.4, 33.1 (cyclohexyl-C), 61.3 (N-CH<sub>2</sub>-C=O), 103.5 (pyridinyl-C<sub>3</sub>), 115.4 (CN), 119.1, 123.1, 127.1, 127.8, 128.3, 129, 132, 135, 135.1, 138.4, 153.9, 156.8, 161.6 (Ar-C) and 168.8 (C=O); IR (KBr, cm<sup>-1</sup>): 3330 (NH), 2236 (CN), 1736 (C=O); Anal. calcd. for C<sub>24</sub>H<sub>19</sub>Cl<sub>2</sub>N<sub>3</sub>O (436.33): C, 66.06; H, 4.39; N, 9.63. Found: C, 66.23; H, 4.34; N, 9.43.

#### 4.1.6. General procedure for the preparation of 1-4-(4-chlorophenyl)-3-cyano-5,6,7,8-tetrahydroquinolin-2-yl)urea or thiourea (**10**, **12**)

A mixture of **1** (1 mmol; 0.28 g) and either urea (5mmol; 0.3 g) or thiourea (5 mmol; 0.4 g) was fused at 180-200°C using a sand bath for 1 h. The reaction mixture was cooled then triturated with ethanol. The obtained solid was filtered, washed several times with water, dried and recrystallized from dimethylformamide/water.

#### 4.1.6.1. 1-4-(4-chlorophenyl)-3-cyano-5,6,7,8-tetrahydroquinolin-2-yl)urea (**10**)

Yellow crystals (0.25 g, 76%); m.p. 180-182°C. <sup>1</sup>H-NMR (300 MHz, [D<sub>6</sub>]DMSO): δ 1.24-1.87 (m, 4H, C<sub>6</sub>-H<sub>2</sub> and C<sub>7</sub>-H<sub>2</sub>), 2.29-2.35 (t, *J* = 9 Hz, 2H, C<sub>5</sub>-H<sub>2</sub>), 3.00-3.06 (t, *J* = 9 Hz, 2H, C<sub>8</sub>-H<sub>2</sub>), 7.08-7.52 (m, 4H, Ar-H), 8.20 (s, 2H, NH<sub>2</sub>, D<sub>2</sub>O-exchangeable) and 9.42 (s, 1H, NH, D<sub>2</sub>O-exchangeable); <sup>13</sup>C-NMR (75 MHz, [D<sub>6</sub>]DMSO): δ 22.2, 22.5, 25.8, 33.3 (cyclohexyl-C), 88.8 (pyridinyl-C<sub>3</sub>), 116.4 (CN), 127.8, 128.3, 128.6, 129.2, 136.2, 153.9 (Ar-C), 156.1 (C=O) and 160.3, 163.5 (pyridinyl-C<sub>2</sub> and C<sub>6</sub>); IR (KBr, cm<sup>-1</sup>): 3334 (NH<sub>2</sub>), 3266 (NH), 2221 (CN), 1691 (C = O); Anal. calcd. for C<sub>17</sub>H<sub>15</sub>ClN<sub>4</sub>O (326.78): C, 62.48; H, 4.63; N, 17.15. Found: C, 62.23; H, 4.46; N, 17.08.

#### 4.1.6.2. 1-4-(4-chlorophenyl)-3-cyano-5,6,7,8-tetrahydroquinolin-2-yl)thiourea (**12**)

Yellow crystals (0.28 g, 83%); m.p. 206-208°C. <sup>1</sup>H-NMR (300 MHz, [D<sub>6</sub>]DMSO): δ 1.66-1.84 (m, 4H, C<sub>6</sub>-H<sub>2</sub> and C<sub>7</sub>-H<sub>2</sub>), 2.43-2.53 (t, *J* = 9.6 Hz, 2H, C<sub>5</sub>-H<sub>2</sub>), 2.89-2.96 (t, *J* = 9.6 Hz, 2H, C<sub>8</sub>-H<sub>2</sub>), 4.03 (s, 2H,

NH<sub>2</sub>, D<sub>2</sub>O-exchangeable), 7.32-7.57 (m, 4H, Ar-H), and 11.84 (s, 1H, NH, D<sub>2</sub>O-exchangeable); <sup>13</sup>C-NMR (75 MHz, [D<sub>6</sub>]DMSO): δ 22.1, 22.5, 25.9, 33.2 (cyclohexyl-C), 88.9 (pyridinyl-C<sub>3</sub>), 114 (CN), 127.9, 128.2, 128.7, 129.1, 136.3, 154 (Ar-C), and 160.2, 164 (pyridinyl-C<sub>2</sub> and C<sub>6</sub>) and 185 (C=S); IR (KBr, cm<sup>-1</sup>): 3432 (NH<sub>2</sub>), 3266 (NH), 2221 (CN), 1214 (C=S); Anal. calcd. for C<sub>17</sub>H<sub>15</sub>ClN<sub>4</sub>S (342.85): C, 59.56; H, 4.41; N, 16.34. Found: C, 59.29; H, 4.43; N, 16.15.

#### 4.1.7. General procedure for the preparation of 4-amino-5-(4-chlorophenyl)-6,7,8,9-tetrahydropyrimido[4,5-b]quinolin-2(1H)-one (11, 13)

A mixture of **1** (1 mmol; 0.28 g) and either urea (5 mmol; 0.3 g) or thiourea (5 mmol; 0.4 g) was fused at 280°C using a sand bath for 1 h. The reaction mixture was cooled then triturated with ethanol. The obtained solid was filtered, washed several times with water, dried and recrystallized from dimethylformamide/water.

##### 4.1.7.1. 4-amino-5-(4-chlorophenyl)-6,7,8,9-tetrahydropyrimido[4,5-b]quinolin-2(1H)-one (11)

Brown crystals (0.21 g, 64%); m.p. 195-197°C. <sup>1</sup>H-NMR (300 MHz, CDCl<sub>3</sub>): δ 1.69-1.89 (m, 4H, C<sub>6</sub>-H<sub>2</sub> and C<sub>7</sub>-H<sub>2</sub>), 2.35-2.42 (t, *J* = 10.5 Hz, 2H, C<sub>5</sub>-H<sub>2</sub>), 3.11-3.17 (t, *J* = 10.5 Hz, 2H, C<sub>8</sub>-H<sub>2</sub>), 7.09-7.47 (m, 4H, Ar-H), 7.77 (s, 2H, NH<sub>2</sub>, D<sub>2</sub>O-exchangeable) and 11.01 (s, 1H, NH, D<sub>2</sub>O-exchangeable); <sup>13</sup>C-NMR (75 MHz, [D<sub>6</sub>]DMSO): δ 21.6, 21.8, 24, 26.9 (cyclohexyl-C), 112.0, 127.7, 128.5, 129.3, 130.6, 132.1, 133.7, 150.4, 156, 159.6, 160.2, 160.9 (Ar-C and C=O); IR (KBr, cm<sup>-1</sup>): 3346 (NH<sub>2</sub>), 3234 (NH), 1691 (C = O); Anal. calcd. for C<sub>17</sub>H<sub>15</sub>ClN<sub>4</sub>O (326.78): C, 62.48; H, 4.63; N, 17.15. Found: C, 62.34; H, 4.55; N, 17.26.

##### 4.1.7.2. 4-amino-5-(4-chlorophenyl)-6,7,8,9-tetrahydropyrimido[4,5-b]quinolin-2(1H)-thione (13)

Brown crystals (0.25 g, 74%); m.p. 226-228°C. <sup>1</sup>H-NMR (300 MHz, [D<sub>6</sub>]DMSO): δ 1.59-1.84 (m, 4H, C<sub>6</sub>-H<sub>2</sub> and C<sub>7</sub>-H<sub>2</sub>), 2.22-2.25 (dist. t, 2H, C<sub>5</sub>-H<sub>2</sub>), 2.95-2.98 (dist. t, 2H, C<sub>8</sub>-H<sub>2</sub>), 7.21-7.50 (m, 6H, Ar-H and NH<sub>2</sub>, D<sub>2</sub>O-exchangeable) and 13.68 (s, 1H, NH, D<sub>2</sub>O-exchangeable); <sup>13</sup>C-NMR (75 MHz, [D<sub>6</sub>]DMSO): δ 20.6, 21.3, 24.8, 26.8 (cyclohexyl-C), 112.0, 127.7, 128.5, 129.3, 130.6, 132.1, 133.7, 150.4, 159.6, 160.2, 160.9 (Ar-C) and 181.9 (C=S); IR (KBr, cm<sup>-1</sup>): 3443 (NH<sub>2</sub>), 3265 (NH), 1234 (C=S); Anal. calcd. for C<sub>17</sub>H<sub>15</sub>ClN<sub>4</sub>S (342.85): C, 59.56; H, 4.41; N, 16.34. Found: C, 59.38; H, 4.31; N, 16.44.

## 4.2. Biological evaluation

### 4.2.1. Animals

Frogs for the *in vitro* AChE testing were obtained from a local supplier, used within 2 days of their purchase. The frogs were kept hydrated throughout the 2 days. Male albino rats (weighing 250-330 g) for the *in vivo* AChE and hepatotoxicity testing were obtained from the animal house of Beirut Arab University. The animals were housed under standard conditions as per the rules and regulations of the Faculty animal ethics committee (IRB) (approval code 2014A-002-P-R-0004)

### 4.2.2. *In vitro* AChE inhibitory activity

All synthesized compounds were evaluated for their *in-vitro* AChE inhibitory effects on acetylcholine-induced contractions of the frog rectus abdominis. After isolation of the triangular muscle of the frog was performed, it was suspended in an organ bath of 10 mL capacity containing aerated Ringer's solution which has been kept at room temperature. The contractions induced by acetylcholine (at a dose of 65  $\mu\text{g}/\text{mL}$ ) were recorded by a force-displacement transducer connected to a Kymograph recorder. The submaximal dose of acetylcholine was determined after a contact time of 1.5 minutes in 3 minute cycles. The solution of the tested compounds in DMF (1  $\mu\text{mol}/\text{mL}$ ) was added 10 minutes before adding the submaximal dose of acetylcholine. Five observations were recorded for each compound.

Calculations of the percentage inhibition of acetyl cholinesterase activity, as indicated by the percentage potentiation of acetylcholine-induced contractions, together with the standard deviation were done and recorded in Table 1.

#### **4.2.3. *In-vivo* acetyl cholinesterase inhibitory activity**

The rats were fasted overnight then given the solutions of the tested compounds at a dose 1 $\mu\text{mol}/\text{Kg}$  body weight, via intraperitoneal route. One hour after drug administration, the rats were sacrificed by decapitation. The whole brain of each rat was removed, immediately and homogenized in 9 volumes of ice-cold 0.1M sodium-potassium phosphate buffer (pH 8.0). The homogenate was centrifuged at 5000 rpm for 30 min. The resultant supernatant was used for estimation of cholinesterase activity spectrophotometrically as reported by Ellman et al [41].

##### **4.2.3.1. Measurement of AChE activity**

Acetyl thiocholine reaction was accomplished by mixing 0.1 mL of the brain homogenate supernatant with 0.5 mM acetyl thiocholine and 0.33 mM 5,5'-dithiobis(2-nitrobenzoic acid) "DTNB" in phosphate buffer (pH 8.0). The intensity of the colored disulfide product resulting from the reaction of the free thiocholine with the Ellman reagent "DTNB" was measured kinetically over 10 min at 412 nm, using a Perkin Elmer type (Lambda 2S) spectrophotometer. Five readings were recorded for each compound. The percent inhibition of acetyl cholinesterase activity and standard deviation were calculated and recorded in Table 1.

#### **4.2.4. Hepatotoxicity testing**

##### **4.2.4.1. Alanine transaminase (ALT) "Serum glutamic pyruvated transaminase (SGPT)" assay**

The rats were given the solutions of the tested compounds in dimethylformamide, in a concentration of 7 mg/Kg body weight, via intraperitoneal route. Control animals were given dimethylformamide or saline. 24 Hours after administering the drug, a blood sample was collected in sterilized dry centrifuge tube and allowed to coagulate for 10 minutes at 37<sup>0</sup>C. The clear serum was separated at 6000 rpm for 10 minutes and subjected to biochemical investigation of SGPT. The kit used was obtained from Medilab (Beirut, Lebanon) and contains L-Alanine, buffer pH7.8, NADH, LDH and oxoglutarate.

The reaction was performed by mixing 0.1 mL of the serum sample with 1 mL of the reconstituted kit. The produced solution was well mixed resulting in a colored product whose intensity was measured at 340 nm, using a Perkin Elmer type (Lambda 2S) spectrophotometer. Five readings were recorded for each compound. The values are recorded in Table 1.

#### 4.2.4.2. Reduced glutathione (GSH) assay

The rats were given the solutions of the tested compounds in dimethylformamide, in a concentration of 7 mg/Kg body weight, via intraperitoneal route. Control animals were given dimethylformamide or saline. 24 Hours after drug administration, the abdomen of each rat was opened and one lobe of the liver was quickly removed, and immediately homogenized in 9 volumes of ice-cold phosphate buffer (0.1 M, pH 8) for GSH measurement.

The reaction was affected by mixing 0.5 ml of the homogenate with 0.5 mL of the precipitating solution followed by centrifugation at 2000 rpm for 5 min. To 0.2 mL of the resulting supernatant, 1.7 mL phosphate buffer (0.1 M, pH 8) and 0.1 mL Ellman reagent were added giving a colored product whose intensity was measured at 412 nm, using a Perkin Elmer type (Lambda 2S) spectrophotometer. The concentration of GSH in the test samples was expressed  $\mu\text{g/mL}$  using standard curve constructed using a serial dilution of GSH. Five readings were recorded for each compound. The values are recorded in Table 1.

#### 4.2.5. Experimental determination of LogP.

The reference substances, benzoic acid, toluene, anthraquinone and benzyl benzoate were dissolved in HPLC grade methanol. Their retention time on RP-C18 column was determined. The HPLC analysis employed reversed-phase C18 column (Agilent HC-C18(2), 5  $\mu\text{m}$ , 150 mm x 4.6 mm, Agilent Technologies, Inc., USA) using photodiode detector (Agilent 1260 Infinity DAD, Agilent Technologies, Inc., USA). For analysis, an isocratic mobile phase of 3:1 (v/v) methanol and water was employed. A volume of 20.0  $\mu\text{L}$  (Agilent 1260 Infinity High performance autosampler) was injected with a flow rate of 0.6 mL/min (Agilent 1260 Infinity Quaternary Pump). Temperature of the column oven was kept at 25  $^{\circ}\text{C}$  (Agilent 1260 Infinity Thermostatted Column Compartment). A calibration curve of  $\log k$  versus  $\log P$  of the reference compounds was constructed to obtain its regression equation. The test compound dissolved in the mobile phase as a solvent was injected into the column. The partition coefficient of the test compound was calculated from interpolation its capacity factor value in the calibration curve regression equation.  $\log P$  of the tested compounds was calculated by extrapolating its  $t_{\text{R}}$  using regression equation ( $r^2 = 0.955$ ). Three readings were recorded for each compound. The values are recorded in Table 2.

#### 4.3. Docking study

Computer-assisted simulation docking experiments were carried out under an MMFF94X force field using Molecular Operating Environment (MOEDock 2009) software, Chemical Computing Group, Montreal, QC.

##### *Docking protocol*

The coordinates from the X-ray crystal structure of AChE used in this simulation were obtained from the Protein Data Bank (PDB ID: 6g1u), where the active site is bound to the inhibitor tacrine derivative 6-chloroanyl-10-methyl-1,2,3,4-tetrahydroacridin-10-ium-9-amine. The ligand molecules were constructed using the builder molecule and were energy minimized. The active site of AChE was generated using the MOE-Alpha Site Finder, and then ligand was docked within this active site using the MOE Dock. The lowest energy conformation was selected, and the ligand interactions (hydrogen bonding together with other hydrophobic interactions) with AChE were recorded.

## 5. References

1. El-Tombary A, Omar A, Eshba N, Rostom S, Ragab H, Saad E. Synthesis and Acetylcholinesterase Inhibitory Activity of Novel Tetrahydroquinoline and Pyrazolo [3, 4-b]-tetrahydroquinoline Derivatives As Potential Agents for Treatment of Alzheimer's Disease. *ALEXANDRIA JOURNAL OF PHARMACEUTICAL SCIENCES* 22(1), 61 (2008).
2. Mohamed LW, Abuel-Maaty SM, Mohammed WA, Galal MA. Synthesis and biological evaluation of new oxopyrrolidine derivatives as inhibitors of acetyl cholinesterase and  $\beta$  amyloid protein as anti-Alzheimer's agents. *Bioorganic chemistry* 76 210-217 (2018).
3. Liu W, Lang M, Youdim MB *et al.* Design, synthesis and evaluation of novel dual monoamine-cholinesterase inhibitors as potential treatment for Alzheimer's disease. *Neuropharmacology* 109 376-385 (2016).
4. Yeong KY, Liew W-L, Murugaiyah V, Ang CW, Osman H, Tan SC. Ethyl nitrobenzoate: A novel scaffold for cholinesterase inhibition. *Bioorganic chemistry* 70 27-33 (2017).
5. Ragab HM, Ashour HM, Galal A, Ghoneim AI, Haïdar HR. Synthesis and biological evaluation of some tacrine analogs: study of the effect of the chloro substituent on the acetylcholinesterase inhibitory activity. *Monatshefte für Chemie-Chemical Monthly* 147(3), 539-552 (2016).
6. Gurjar AS, Darekar MN, Yeong KY, Ooi L. In silico studies, synthesis and pharmacological evaluation to explore multi-targeted approach for imidazole analogues as potential cholinesterase inhibitors with neuroprotective role for Alzheimer's disease. *Bioorganic & medicinal chemistry* (2018).
7. Mayo foundation for medical education and research. <http://www.Mayoclinic.com.htm>. (June 2018).
8. Brody TM, Larner J, Minneman KP, Wecker L. *Brody's human pharmacology: molecular to clinical*. Elsevier Mosby, (2005).
9. Rang HP. Rang and Dale's pharmacology. *Churchill Livingstone Elsevier* 727 (2007).
10. Joubert J, Foka GB, Repsold BP, Oliver DW, Kapp E, Malan SF. Synthesis and evaluation of 7-substituted coumarin derivatives as multimodal monoamine oxidase-B and cholinesterase inhibitors for the treatment of Alzheimer's disease. *European journal of medicinal chemistry* 125 853-864 (2017).
11. Vafadarnejad F, Mahdavi M, Karimpour-Razkenari E *et al.* Design and synthesis of novel coumarin-pyridinium hybrids: In vitro cholinesterase inhibitory activity. *Bioorganic chemistry* 77 311-319 (2018).
12. Hardy J. The amyloid hypothesis for Alzheimer's disease: a critical reappraisal. *Journal of neurochemistry* 110(4), 1129-1134 (2009).
13. Webber KM, Raina AK, Marlatt MW *et al.* The cell cycle in Alzheimer disease: a unique target for neuropharmacology. *Mechanisms of ageing and development* 126(10), 1019-1025 (2005).
14. Więckowska A, Kołaczkowski M, Bucki A *et al.* Novel multi-target-directed ligands for Alzheimer's disease: Combining cholinesterase inhibitors and 5-HT<sub>6</sub> receptor antagonists. Design, synthesis and biological evaluation. *European journal of medicinal chemistry* 124 63-81 (2016).
15. Zemek F, Drtinova L, Nepovimova E *et al.* Outcomes of Alzheimer's disease therapy with acetylcholinesterase inhibitors and memantine. *Expert opinion on drug safety* 13(6), 759-774 (2014).

16. Rizzo S, RivièRe CL, Piazzì L *et al.* Benzofuran-based hybrid compounds for the inhibition of cholinesterase activity,  $\beta$  amyloid aggregation, and A $\beta$  neurotoxicity. *Journal of medicinal chemistry* 51(10), 2883-2886 (2008).
17. Saeed A, Mahesar PA, Zaib S *et al.* Synthesis, cytotoxicity and molecular modelling studies of new phenylcinnamide derivatives as potent inhibitors of cholinesterases. *European journal of medicinal chemistry* 78 43-53 (2014).
18. Ragab HM, Kim JS, Dukat M, Navarro H, Glennon RA. Aryloxyethylamines: Binding at  $\alpha$ 7 nicotinic acetylcholine receptors. *Bioorganic & medicinal chemistry letters* 16(16), 4283-4286 (2006).
19. De Souza LG, Rennó MN, Figueroa-Villar JD. Coumarins as cholinesterase inhibitors: a review. *Chemico-biological interactions* 254 11-23 (2016).
20. Sang Z, Wang K, Wang H *et al.* Design, synthesis and biological evaluation of phthalimide-alkylamine derivatives as balanced multifunctional cholinesterase and monoamine oxidase-B inhibitors for the treatment of Alzheimer's disease. *Bioorganic & medicinal chemistry letters* 27(22), 5053-5059 (2017).
21. Rayatzadeh A, Saeedi M, Mahdavi M *et al.* Synthesis and evaluation of novel oxoisindoline derivatives as acetylcholinesterase inhibitors. *Monatshefte für Chemie-Chemical Monthly* 146(4), 637-643 (2015).
22. Saeed A, Zaib S, Ashraf S *et al.* Synthesis, cholinesterase inhibition and molecular modelling studies of coumarin linked thiourea derivatives. *Bioorganic chemistry* 63 58-63 (2015).
23. Elumalai K, Ali MA, Munusamy S, Elumalai M, Eluri K, Srinivasan S. Novel pyrazinamide condensed azetidiones inhibit the activities of cholinesterase enzymes. *Journal of Taibah University for Science* 10(5), 643-650 (2016).
24. Sarfraz M, Sultana N, Rashid U, Akram MS, Sadiq A, Tariq MI. Synthesis, biological evaluation and docking studies of 2, 3-dihydroquinazolin-4 (1H)-one derivatives as inhibitors of cholinesterases. *Bioorganic chemistry* 70 237-244 (2017).
25. Romero A, Cacabelos R, Oset-Gasque MJ, Samadi A, Marco-Contelles J. Novel tacrine-related drugs as potential candidates for the treatment of Alzheimer's disease. *Bioorganic & medicinal chemistry letters* 23(7), 1916-1922 (2013).
26. Liu Z, Fang L, Zhang H, Gou S, Chen L. Design, synthesis and biological evaluation of multifunctional tacrine-curcumin hybrids as new cholinesterase inhibitors with metal ions-chelating and neuroprotective property. *Bioorganic & medicinal chemistry* 25(8), 2387-2398 (2017).
27. Khoobi M, Ghanoni F, Nadri H *et al.* New tetracyclic tacrine analogs containing pyrano [2, 3-c] pyrazole: efficient synthesis, biological assessment and docking simulation study. *European journal of medicinal chemistry* 89 296-303 (2015).
28. Martins C, Carreiras MC, León R *et al.* Synthesis and biological assessment of diversely substituted furo [2, 3-b] quinolin-4-amine and pyrrolo [2, 3-b] quinolin-4-amine derivatives, as novel tacrine analogues. *European journal of medicinal chemistry* 46(12), 6119-6130 (2011).
29. Soukup O, Jun D, Zdarova-Karasova J *et al.* A resurrection of 7-MEOTA: a comparison with tacrine. *Current Alzheimer Research* 10(8), 893-906 (2013).
30. Alldredge BK, Corelli RL, Ernst ME, Guglielmo B, Jacobson P, Kradjan W. Koda-Kimble & Young's applied therapeutics. (2013).
31. Erdelyi M. Halogen bonding in solution. *Chemical Society Reviews* 41(9), 3547-3557 (2012).
32. Gregor VE, Emmerling MR, Lee C, Moore CJ. The synthesis and in vitro acetylcholinesterase and butyrylcholinesterase inhibitory activity of tacrine (Cognex<sup>®</sup>) derivatives. *Bioorganic & medicinal chemistry letters* 2(8), 861-864 (1992).

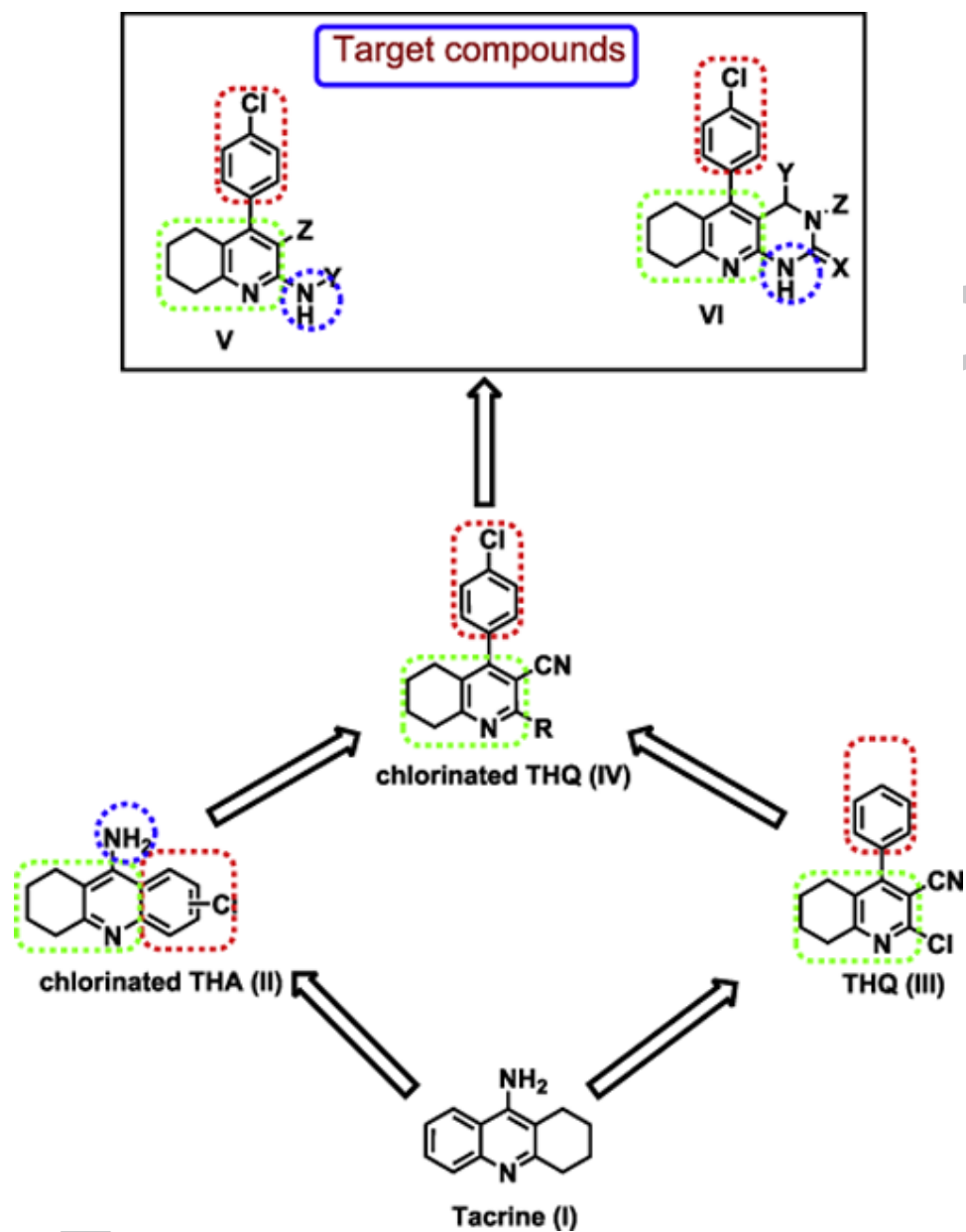
33. Reddy EK, Remya C, Mantosh K *et al.* Novel tacrine derivatives exhibiting improved acetylcholinesterase inhibition: Design, synthesis and biological evaluation. *European journal of medicinal chemistry* 139 367-377 (2017).
34. Molsoft. <http://molsoft.com/mprop>. (June 2018).
35. Preadmet. <http://preadmet.bmdrc.org>. (June 2018).
36. Molinspiration. <http://www.molinspiration.com>. (June 2018).
37. Kambe S, Saito K, Sakurai A, Midorikawa H. A simple method for the preparation of 2-amino-4-aryl-3-cyanopyridines by the condensation of malononitrile with aromatic aldehydes and alkyl ketones in the presence of ammonium acetate. *Synthesis* 1980(05), 366-368 (1980).
38. Wan Y, Yuan R, Zhang F-R *et al.* One-pot synthesis of N2-substituted 2-amino-4-aryl-5, 6, 7, 8-tetrahydroquinoline-3-carbonitrile in basic ionic liquid [bmim] OH. *Synthetic Communications* 41(20), 2997-3015 (2011).
39. Barlow R, Crawford T, Perry W. Pharmacological experiments on isolated preparations. *Churchill Livingstone, New York* 58 (1974).
40. Brunton LL, Chabner B, Knollmann BC. Goodman & Gilman's the pharmacological basis of therapeutics. (2011).
41. Ellman GL, Courtney KD, Andres Jr V, Featherstone RM. A new and rapid colorimetric determination of acetylcholinesterase activity. *Biochemical pharmacology* 7(2), 88-95 (1961).
42. Burtis CA, Bruns DE. *Tietz Fundamentals of Clinical Chemistry and Molecular Diagnostics-E-Book*. Elsevier Health Sciences, (2014).
43. Kumar R, Kumar A, Sharma R, Baruwala A. Pharmacological review on natural ACE inhibitors. *Der Pharmacia Lettre* 2(2), 273-293 (2010).
44. Raju NJ, Sreekanth N. Investigation of hepatoprotective activity of *Ficus retusa* (Moraceae). *International Journal of Research in Ayurveda and Pharmacy (IJRAP)* 1(1), 166-169 (2010).
45. Ganesan K, Sukalingam K, Xu B. Solanum trilobatum L. Ameliorate Thioacetamide-Induced Oxidative Stress and Hepatic Damage in Albino Rats. *Antioxidants* 6(3), 68 (2017).
46. Madden S, Woolf TF, Pool WF, Park BK. An investigation into the formation of stable, protein-reactive and cytotoxic metabolites from tacrine in vitro: studies with human and rat liver microsomes. *Biochemical pharmacology* 46(1), 13-20 (1993).
47. Park SM, Ki SH, Han NR *et al.* Tacrine, an oral acetylcholinesterase inhibitor, induced hepatic oxidative damage, which was blocked by liquiritigenin through GSK3-beta inhibition. *Biological and Pharmaceutical Bulletin* 38(2), 184-192 (2015).
48. Bose PP, Chatterjee U, Hubatsch I *et al.* In vitro ADMET and physicochemical investigations of poly-N-methylated peptides designed to inhibit A $\beta$  aggregation. *Bioorganic & medicinal chemistry* 18(16), 5896-5902 (2010).
49. Mälkiä A, Murtomäki L, Urtti A, Kontturi K. Drug permeation in biomembranes: in vitro and in silico prediction and influence of physicochemical properties. *European Journal of Pharmaceutical Sciences* 23(1), 13-47 (2004).
50. Cheng F, Li W, Zhou Y *et al.* admetSAR: a comprehensive source and free tool for assessment of chemical ADMET properties. (2012).
51. Ntie-Kang F, Onguéné PA, Lifongo LL, Ndom JC, Sippl W, Mbaze LMA. The potential of anti-malarial compounds derived from African medicinal plants, part II: a pharmacological evaluation of non-alkaloids and non-terpenoids. *Malaria journal* 13(1), 81 (2014).
52. Pajouhesh H, Lenz GR. Medicinal chemical properties of successful central nervous system drugs. *NeuroRx* 2(4), 541-553 (2005).

53. Brain penetration (work in progress). [https://www.cambridgemedchemconsulting.com/resources/ADME/brian\\_penetration.html](https://www.cambridgemedchemconsulting.com/resources/ADME/brian_penetration.html). (february 2019).
54. Abdelsalam MA, Aboulwafa OM, M Badawey E-SA *et al.* Design, synthesis, anticancer screening, docking studies and in silico ADME prediction of some  $\beta$ -carboline derivatives. *Future medicinal chemistry* (0), (2018).
55. Valkó K. Application of high-performance liquid chromatography based measurements of lipophilicity to model biological distribution. *Journal of chromatography A* 1037(1-2), 299-310 (2004).
56. Galdeano C, Coquelle N, Cieslikiewicz-Bouet M *et al.* Increasing Polarity in Tacrine and Huprine Derivatives: Potent Anticholinesterase Agents for the Treatment of Myasthenia Gravis. *Molecules* 23(3), 634 (2018).
57. Maharani S, Almansour AI, Kumar RS, Arumugam N, Kumar RR. Synthesis of cycloalkano [b] pyridines by multicomponent strategy: ring-size mediated product selectivity, substitution-induced axial chirality and influence of the 14 N quadrupole-relaxation. *Tetrahedron* 72(30), 4582-4592 (2016).
58. El-Salam O, Ella D, Ismail N, Abdullah M. Synthesis, docking studies and anti-inflammatory activity of some 2-amino-5, 6, 7, 8-tetrahydroquinoline-3-carbonitriles and related compounds. *Die Pharmazie-An International Journal of Pharmaceutical Sciences* 64(3), 147-155 (2009).

**Highlights**

- Chlorinated tacrine analogs were designed, synthesized and evaluated for their *in vitro* and *in vivo* anti-cholinesterase activity.
- All compounds showed activities either comparable to or significantly higher than tacrine.
- Hepatotoxicity of compounds was evaluated by determining SGPT and reduced GSH levels and the results indicated that all compounds showed a safe hepatic profile.
- *In silico* physicochemical characters and pharmacokinetic parameters together with practical logP testing were assessed indicating that all synthesized compounds are promising hits/leads for treatment of Alzheimer's disease.

Graphical abstract



SCRIPT

A